VOLUME 30 MAY 1952 NUMBER 5

Canadian Journal of Chemistry

Editor: J. W. T. SPINKS

Published by THE NATIONAL RESEARCH COUNCIL
OTTAWA CANADA

CANADIAN JOURNAL OF CHEMISTRY

(Formerly Section B, Canadian Journal of Research)

The CANADIAN JOURNAL OF CHEMISTRY is published monthly by the National Research Council of Canada under the authority of the Chairman of the Committee of the Privy Council on Scientific and Industrial Research. Matters of general policy are the responsibility of a joint Editorial Board consisting of members of the National Research Council of Canada and the Royal Society of Canada.

The National Research Council of Canada publishes also: *Canadian Journal of Botany, Canadian Journal of Medical Sciences, Canadian Journal of Physics, Canadian Journal of Technology, Canadian Journal of Zoology.*

The CANADIAN JOURNAL OF CHEMISTRY and the CANADIAN JOURNAL OF TECHNOLOGY have been chosen by the Chemical Institute of Canada as its medium of publication for scientific papers.

EDITORIAL BOARD

Representing
NATIONAL RESEARCH COUNCIL

DR. J. H. L. JOHNSTONE (*Chairman*),
Professor of Physics,
Dalhousie University,
Halifax, N.S.

DR. OTTO MAASS,
Macdonald Professor of
Physical Chemistry,
McGill University,
Montreal, P.Q.

DR. CHARLES W. ARGUE,
Dean of Science,
University of New Brunswick,
Fredericton, N.B.

DR. A. G. MCCALLA,
Dean, Faculty of Agriculture
University of Alberta,
Edmonton, Alta.

Ex officio

DR. LÉO MARION (*Editor-in-Chief*),
Director, Division of Pure Chemistry,
National Research Laboratories,
Ottawa.

DR. H. H. SAUNDERSON,
Director, Division of Information Services,
National Research Council,
Ottawa.

Representing
ROYAL SOCIETY OF CANADA

Section III

DR. G. M. VOLKOFF,
Professor of Physics,
University of British Columbia,
Vancouver, B.C.

DR. J. W. T. SPINKS,
Dean, College of Graduate
Studies,
University of Saskatchewan,
Saskatoon, Sask.

Section V

DR. H. S. JACKSON,*
Head, Department of Botany,
University of Toronto,
Toronto, Ont.

DR. E. HORNE CRAIGIE,
Department of Zoology,
University of Toronto,
Toronto, Ont.

Representing
THE CHEMICAL INSTITUTE OF CANADA

DR. H. G. THODE,
Department of Chemistry
McMaster University,
Hamilton, Ont.

Manuscripts should be addressed to:

DR. LÉO MARION,
Editor-in-Chief,
Canadian Journal of Chemistry,
National Research Council,
Ottawa, Canada.

Each manuscript should be typewritten, double-spaced, and the original and one extra copy submitted (see **Notice to Contributors** inside of back cover).

Subscriptions, renewals, and orders for back numbers should be addressed to:

Administrative Services,
National Research Council,
Ottawa, Canada.

Subscription rate: $4.00 a year; single numbers: 50 cents. Special rates can be obtained for subscriptions to more than one of the Journals published by the National Research Council.

*Deceased.

Canadian Journal of Chemistry

Issued by THE NATIONAL RESEARCH COUNCIL OF CANADA

VOLUME 30 MAY, 1952 NUMBER 5

THE FLOW OF FLUIDS THROUGH ACTIVATED CARBON RODS

III. THE FLOW OF ADSORBED FLUIDS[1*]

BY E. A. FLOOD, R. H. TOMLINSON, AND A. E. LEGER

ABSTRACT

Total flow rates of gases through activated charcoal rods are regarded as consisting of the sums of comparatively independent flows through macropores and micropores. The flow rate through the macropore system is related to the relevant adsorption isotherm by means of an empirical equation having three arbitrary constants. The empirical equations can be fitted to all of our observed results within the experimental error. Assuming that the adsorbate behaves as a one-component fluid such as a gas in a gravitational field, it is shown that compressive surface forces give rise to large fluid pressures within micropores. A very simple flow equation is derived which is qualitatively in agreement with observed results and which indicates a mean micropore diameter of the order of 10^{-7} cm. The derived equation illustrates the nature of the physical factors involved and shows that surface forces may increase flow rates of adsorbable gases by very large factors. The increased flow rates are dué mainly to the greatly increased densities and to the increased pressure gradients resulting from the action of surface forces. A model porous adsorbent is presented which exhibits many properties of real adsorbent systems and illustrates especially the relations between adsorbate densities and the various tensions and pressures existing within micropore systems.

GENERAL CONSIDERATIONS

The flow rate in mass units, Q_m, of a Maxwellian fluid through a pipe of circular cross section may be described by the equation,

$$Q_m = -\frac{\pi r^4}{8\eta}\rho\left(1 + \frac{4\xi}{r}\right)\frac{dp}{dz}, \tag{1}$$

where dp/dz is the pressure gradient at any point along the axis of the pipe; r, the radius of the pipe; ρ, the density of the fluid; η, its viscosity; and ξ is the coefficient of slip.

Maxwell's treatment of the "slip" phenomenon as interpreted by Kennard (6) leads to the following expression,

$$f\left(\frac{1}{2}\eta\frac{dv_0}{dx} + \frac{1}{4}n\bar{v}mv_s\right) = \eta\frac{dv_0}{dx} \tag{2}$$

where f is the fraction of the tangential momentum brought up to the surface of the pipe per second which is actually transferred to the surface (thus f cannot exceed two and under any reasonably probable condition will not

[1] *Manuscript received August 16, 1951.*
Contribution from the Division of Chemistry, National Research Council, Ottawa, Canada. Issued as N.R.C. No. 2705.

* *Parts I and II of this series appeared in the April issue of this Journal (Can. J. Chem. 30: 348; 372. 1952). These papers are referred to in this paper as "Parts I and II".*

exceed one), dv_0/dx is the velocity gradient, v_s is the slip velocity and is equal to $-\xi\, dv_0/dx$, n is the number of molecules per unit volume, $\bar{v}$ is their mean speed, and m their mass. From (2) ξ is given by,

$$\xi = \frac{\eta}{\rho}\sqrt{\frac{\pi M}{2RT}}\cdot\frac{2-f}{f}. \tag{3}$$

While in the case of liquids it is customary to neglect slip altogether, we might by an argument similar to that used above arrive at an analogous expression for liquid slip. In this case, the much greater rate of transfer of momentum consistent with the rate of diffusion of mass will require the introduction of factors which largely invalidate the simple treatment. However, since $\eta dv/dx$ is a measure of the shearing force in liquids as well as in gases, we will write for the coefficient of slip for both liquids and gases,

$$\xi = \gamma\frac{\eta}{\rho}\sqrt{\frac{\pi M}{2RT}},$$

where we may take γ as approximately unity in the case of gases and where we estimate γ to be not greater than 10^{-3} for Newtonian liquids whose viscosities are of the order of one centipoise and which wet the walls of the pipe.*

With these assumptions the laminar flow rate in K units for either gas or liquid may be written,

$$K = \frac{\pi r^4}{8\eta L}\bar{\rho}\frac{RT}{M} + \gamma\frac{\pi r^3}{2L}\sqrt{\frac{\pi RT}{2M}}, \tag{4}$$

there $\bar{\rho}$ is the mean density of the fluid over the pressure interval Δp. If the fluid is a liquid, ρ is practically independent of p, i.e., $\bar{\rho}$ is just the liquid density. In the case of liquid flow, the mass flow per second is converted to gas flow in volume units per second, the volumes being assumed measured at some arbitrary low pressure where the vapor obeys the ideal gas laws, and the flow in K units is calculated for the appropriate pressures.†

In the case of many common volatile liquids, ρ/η is upwards of 10 times that of the corresponding term for their saturated vapors, hence terms in r^4 for liquids are upwards of 10 times the corresponding terms for their saturated vapors. The actual ratios depend, of course, on the particular values of the

*ξ *is probably negative in many cases, cf. Part I of this series of papers.*

†*For liquids where* $\rho \to 1$, $\eta \to 10^{-2}$, $\sqrt{\frac{RT}{M}} \to 10^4$, *and* $\gamma \to 10^{-3}$, *we can write Equation 4 in the form,* $K = A\,[r(2.3 \times 10^8) + 1]$. *Hence the term in r, the Poiseuille term, is greater than the "slip" term for* $r \geqslant 10^{-8}$. *Since laminar flow cannot take place in capillaries whose diameters are only slightly greater than molecular dimensions, the "slip" term for Newtonian liquids whose viscosities are of the order of one centipoise is probably negligible compared with the Poiseuille term under any ordinary conditions of viscous flow in round or square capillaries regardless of size. In the case of capillaries whose mean apparent radii are of the order of a few Ångstrom units, any flow phenomena will be controlled by the interactions of the fluid with the wall and hence will not be strictly a "slip" flow but rather a limiting type of molecular effusion or a limiting type of surface diffusion. The latter is almost certainly an activated rate process involving relatively large activation energies.*

viscosities and densities and especially on the vapor densities or vapor pressures of the liquids.*

If we represent the liquid laminar flow rate by K_l and the nearly saturated vapor flow rate by K_g, we can estimate the limiting ratio, K_l/K_g, as the density of the saturated vapor becomes small and transport from gaseous viscous flow vanishes. Where the gaseous flow becomes an effusive process, the "slip" and "effusive" flows have the same values in capillaries of suitable length–diameter ratios, i.e., $K_g \rightarrow \frac{\pi r^3}{2L}\sqrt{\frac{\pi RT}{2M}}$. Thus for substances of molecular weight of about 50 which in liquid form have densities of about unity and viscosities of about one centipoise, the limiting ratio, K_l/K_g, as the vapor pressure approaches zero is roughly,

$$\frac{K_l}{K_g} \rightarrow r(10^5 \text{ to } 10^6) + \gamma, \tag{5}$$

where γ is probably not greater than 10^{-3}. If the capillary diameter is much greater than its length, the ratio may be increased by a factor of perhaps 20.

While evidently, in the case of capillaries of radius greater than 10^{-5} cm., liquefaction can cause a marked increase in flow rate as measured in K units, liquefaction will not in general increase flow rates appreciably in capillaries of radius less than 10^{-6} cm., unless other factors than density and viscosity are involved.

In the case of capillaries whose diameters are of the order of those corresponding to the micropore structure of our activated carbon rods ($\lesssim 2 \times 10^{-7}$ cm.†), even if the capillary lengths are much less than their diameters and the gas is compressed to a density comparable with that of the corresponding liquid,

As a rough check on the validity of such relations as applied to small capillaries in regions near saturation, experiments were carried out in which the saturated vapor of a liquid was allowed to flow through the capillary of an imperfectly sealed glass tube. By raising the level of the liquid it was possible to force liquid through the same capillary. The radius and length of capillary passage as calculated from air permeability were 2×10^{-3} and 0.5 cm. respectively. The flow rates observed for acetone, diethyl ether, and carbon tetrachloride, both as liquid and vapor, agreed reasonably well with calculated values. The following diagram (not to scale) illustrates results obtained from acetone.

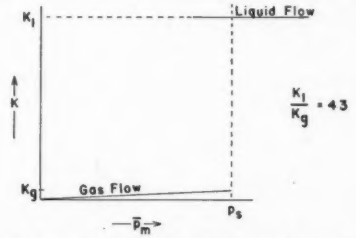

The observed flow rate of liquid acetone was found to be 43 times the flow of its saturated vapor, while the calculated ratio based on handbook data lies between 41 and 42. Similar results were obtained with the other fluids used. It may be remarked that in the case of liquid carbon tetrachloride long thin rods of solid were sometimes formed on the effluent side. Although the cooling due to evaporation must have considerable influence on the rate of flow, evidently in this case the flow rate is controlled by viscous flow.

†*cf. Emmett (3), also Juhola (5).*

the increased flow rate, if any, due to the increased density alone is probably too small to be comparable with the gas flow rates through the macropore system. However, if we suppose that within or in intimate contact with the relatively rough solid surface of the carbon some sort of comparatively independent surface diffusion is taking place and add this flow to a dense gaseous laminar flow within the micropores, we might obtain a total flow rate for the micropore system of the correct order of magnitude. Since the adsorption isotherm affords a measure of the mean fluid density within the micropores, we might, as previously suggested (8), suppose the surface diffusion rate proportional to the density gradient or to the gradient of the ordinate, X, of the adsorption isotherm. Such a procedure leads to an equation for the flow rate which is obviously not in accordance with the data. If, however, we suppose a transport rate proportional to $X^{n-1}\,dX/dz$ rather than to dX/dz, an equation is obtained which can be made to fit the data. Thus, if for the flow rate through the micropore system we write,

$$Q_m = \alpha' X \frac{dp}{dz} + \beta' X^{n-1} \frac{dX}{dz},$$

or, in K units,

$$K = \alpha|\overline{X}|_{\Delta p} + \beta \frac{X_1^{\,n} - X_2^{\,n}}{\Delta p},$$

and this is now added to the flow rate through the macropore system, i.e., to the Adzumi flow, we obtain the following empirical equation,

$$K = \frac{A}{\eta}\bar{p} + \frac{B}{\sqrt{M}} + \alpha|\overline{X}|_{\Delta p} + \beta\frac{X_1^{\,n} - X_2^{\,n}}{\Delta p}, \tag{6}$$

where A and B apply to the macropore system and are to be calculated as indicated in Part II; the terms in α and β apply to the micropore system; $|\overline{X}|_{\Delta p}$ is the mean value of the ordinate of the isotherm over the pressure interval Δp; and X_1 and X_2 are the isotherm ordinates corresponding to p_1 and p_2 respectively. α, β, and n are adjustable constants. As shown in Part I of this paper, Equation 6 fits all of the data probably within the experimental error. The solid lines (*b*) in Figs. 3 to 8 (Part I) are not drawn through the experimental points but are calculated from Equation 6, the "constants" being adjusted for each gas as shown in the figures.

While the agreement between the observed results and those calculated by means of Equation 6 indicates a correlation between flow rate and adsorption behavior, Equation 6 has a number of faults. The large and apparently erratic variation of the constants suggests that the equation does not correlate the physical factors involved correctly. The term in $|\overline{X}|_{\Delta p}$, the controlling term in the case of water, can hardly be due to any ordinary sort of diffusion and, as we have seen, the pore diameters of the micropore system are too small for this to be an ordinary Poiseuille term. Further, it seems improbable that the "diffusion constant" of a dense fluid layer over a relatively rough

surface can be as large as the coefficient of self-diffusion of most common liquids; consequently, it is improbable that anything like an ordinary diffusion rate proportional to the cross-sectional area and to dp/dz or to $\rho^n d\rho/dz$ can be large enough to account for our results in the higher relative pressure ranges. Finally, Equation 6 contains no explicit term involving the structure of the micropore system.

Babbitt (1) and Carman (2) have found somewhat similar anomalous flow rates and have discussed the problems involved in some interesting papers. Carman has used semiempirical relations based on concentration gradients to describe his results and finds a correlation between the adsorption isotherm and the flow rate. But, as he points out, the correlation is not very satisfactory. In place of the concentration gradient, Babbitt has used the "spreading pressure gradient", the spreading pressure being related to the adsorption isotherm by the method of Fowler and Guggenheim (4) as applied to "ideal mobile monolayers" and to "ideal localized monolayers". Babbitt extends his discussion to multilayer adsorption. While we consider that the use of the "spreading pressure" is fundamentally the correct approach to some of these problems, we are inclined to believe that when dealing with thick multilayers the flow is primarily a process of fluid layers sliding over each other and not strictly a "diffusion" phenomenon at all. It is thought that many of the well-known rapid surface-spreading phenomena are primarily laminar flow problems, the rapid spreading being due largely to the development of relatively high drift velocities. The basic notions involved in viscous flow, diffusive flow, etc., require that the relevant proportionality constants be, in fact, roughly constant. If the "viscosity" appeared to vary widely with velocity gradient, pressures, dimensions of apparatus, etc., the flow could hardly be considered as a viscous flow at all. If we allow a "diffusion constant" to vary widely with concentration gradients, the dimensions of the apparatus, and with other factors foreign to the basic notions of diffusive motion, the broadening of the term "diffusion" largely destroys its meaning. When the terms are thus broadly used there is little or no distinction between viscous flow and diffusive flow. Finally, it may be remarked that thermodynamic potential gradients as expressed, say by the appropriate voltage gradients, osmotic pressure gradients, etc., do not necessarily imply that such voltage gradients, pressure gradients, etc. actually exist in the system concerned. Nor are any of these gradients necessarily directly involved in any rate process which may be occurring.

It is, of course, exceedingly improbable that any very exact description of the flow of adsorbed material can be deduced that shall have any generality. However, in the case of activated carbon such as used in our experiments, a great deal of data is available concerning its structure, pore-diameter frequency distributions, and adsorption behavior generally.* From these data a good many reasonably valid inferences can be drawn as to the nature and state of the adsorbate, the magnitudes of the hydrodynamic pressures, etc.

*cf. *Emmett* (3).

Accordingly, it seems worth-while to attempt to deduce from simply thermodynamic and hydrodynamic considerations a correlation between flow rates and adsorptive capacity that shall include the fine structure of the material and that shall be somewhat less arbitrary than Equation 6.

MODEL POROUS ADSORBENT

Before enquiring into the possible effects of compressive surface forces on flow phenomena, we shall discuss some of the more pertinent conditions which prevail when an active adsorbent is exposed to a condensable vapor or when an adsorption measurement is made by the McBain and similar techniques.

During adsorption measurements, in addition to the isothermal condition, the adsorbent as a whole is enveloped in the vapor of the adsorbable gas and accordingly the mean pressure or the hydrostatic pressure of the adsorbent–adsorbate body is equal to that of the hydrostatic envelope. If we have reason to believe that the adsorbent–adsorbate system may be regarded as two distinct bodies of matter, that the adsorbent may be regarded as a fine-grained, isotropic, porous, rigid solid, and that the adsorbate may be regarded as a more or less continuous fluid having the properties of a pure gas or a liquid, it is perfectly self-consistent and possible for the solid and fluid to be under quite different states of compression or tension. While the thermodynamics of such systems have been discussed by many writers, Gibbs, Bangham, Hill, etc., we shall only discuss a very simple highly idealized case. We shall assume that the solid is an incompressible and perfectly rigid isotropic fine-grained porous body having a very low vapor pressure. The solid will be regarded as being uniformly under a characteristic state of tension or compression resulting from the action of attractive forces on the gas and we shall enquire into states of compression of the adsorbate consistent therewith. We assume that we may write for this idealized system the following approximation,

$$V p_H = V_a p_a + V_c p_c \tag{7}*$$

and,

$$p_H = D_1 p_a + D_2 p_c ,$$

where V is the volume of the whole porous system, and p_H is the net mean pressure of the adsorbate–adsorbent system and is the same as that of the hydrostatic envelope of the surrounding gas with which it is in equilibrium. V_a is the pore volume or volume of pure adsorbate, V_c is the volume of the carbon, p_a is the mean pressure of the adsorbate, and p_c is the pressure of the solid or carbon. D_1 and D_2 are respectively V_a/V and V_c/V, and $D_1 + D_2 = 1$. The volume of the "two-component" interface between pure adsorbate and adsorbent (and hence the weight of adsorbable gas contained therein) is assumed to be negligible in comparison with volumes V_a and V_c.

**If we include a void volume having a pressure p_H to correspond with an ideal nonadsorbing macropore system, essentially the same result is obtained as is derived in what follows.*

If the solid exerts an attractive force on the gas molecules tending to concentrate the gas within the pores, then under equilibrium conditions, the adsorbate will in general have a higher density than the gas constituting the hydrostatic envelope. If no surface of discontinuity or meniscus separates the adsorbate from the gas, the pressure p_a will usually be positive and exceed p_H, while the pressure p_c of the solid will be less than p_H and may be negative. If, however, surfaces of discontinuity capable of supporting any very appreciable pressures separate adsorbate from gas, the net pressure of the adsorbate may be positive or negative. When p_a is negative p_c is necessarily positive, i.e., the solid is under a state of compression.

The magnitudes of these pressures may be estimated in a number of ways. We may regard the problem as essentially a membrane equilibrium and apply the relation *

$$Vdp_H = V_{1e}dp_{1e} + V_{2e}dp_{2e}, \tag{8}$$

where V is the total volume of adsorbent-adsorbate system as in Equation 7; p_H its hydrostatic pressure; V_{1e} the volume of pure adsorbate gas (containing the same matter) in equilibrium through a semipermeable membrane, permeable only to pure gaseous adsorbate; V_{2e} the volume of carbon vapor similarly in equilibrium; and p_{1e} and p_{2e} are the corresponding equilibrium pressures.

We may write Equation 8 in the form,

$$dp_H = \frac{x}{u_1}dp_{1e} + \frac{y}{u_2}dp_{2e} \tag{9}$$

where x and y are the apparent densities of adsorbate and solid, respectively, in the porous system. Thus if ρ_a and ρ_c are the actual mean densities of adsorbate and solid respectively, then $x = D_1\rho_a$ and $y = D_2\rho_c$. u_1 and u_2 are the equilibrium vapor densities of pure adsorbable gas and pure vapor of the solid respectively.

If p_{2s} is the vapor pressure of pure adsorbent ($u_1 = 0$, $x = 0$) under a hydrostatic pressure equal to its vapor pressure and the equilibrium gas density is u_{2s}, then assuming the vapor to be an ideal gas and the solid to be incompressible, the equilibrium gas density u_2 of the solid under the hydrostatic pressure p_c will be given by,

$$p_c = \rho_c\frac{RT}{M}\log\frac{u_2}{u_{2s}} + p_{2s}. \tag{10}$$

Integrating Equation 9 from $u_1 = 0$, $u_2 = u_{2s}$ to u_1 and u_2, since y is constant and the pure vapor of the solid is very dilute and is assumed to be an ideal gas, we get,

$$p_H - p_{2s} = \int_{0,u_{2s}}^{u_1,u_2}\frac{x}{u_1}dp_{1e} + y\frac{RT}{M}\log\frac{u_2}{u_{2s}},$$

*Cf. Flood, E. A. and Benson, G. C. *Can. J. Research, B, 27: 988. 1949.*

which combined with Equation 10 gives,

$$p_H - p_{2s} = \int_{0,u_{2s}}^{u_1,u_2} \frac{x}{u_1} dp_{1e} + D_2(p_c - p_{2s})$$

and hence from Equation 7 we get,

$$p_a = \int_{0,u_{2s}}^{u_1,u_2} \frac{\rho_a}{u_1} dp_{1e} + p_{2s} = \left|\overline{\frac{\rho_a}{u_1}}\right|_e p_{1e} + p_{2s}, \tag{11}$$

where $\left|\overline{\rho_a/u_1}\right|_e$ is the average value of ρ_a/u_1 under equilibrium conditions along the path $u_1 = 0$, $u_2 = u_{2s}$ to u_1 and u_2. If the vapor pressure of the solid is very small compared with p_{1e}, p_{1e} becomes indistinguishable from p_H and we can drop the subscripts and write,

$$p_a = \left|\overline{\frac{\rho_a}{u_1}}\right| p,$$

where p is the pressure of the gas in equilibrium with fluid adsorbate whose mean hydrostatic pressure is p_a.*

If phase changes may occur, u_1 and ρ_a may not be defined for a given value of p_{1e}, say, p_{1e}'. Then ρ_a/u_1 will not be defined for p_{1e}'. If, however, u_1 and ρ_a are defined for regions above and below p_{1e}', the mean value of ρ_a/u_1 will still be defined for a finite interval including p_{1e}'.

If above p_{1e}', ρ_a corresponds to the liquid density, while below p_{1e}', ρ_a is much less than the liquid density, so that at p_{1e}' two different density states can coexist, usually we will have a surface of discontinuity or a meniscus form. Once the adsorbate volume is full of liquid, if the meniscus has an appreciable surface energy (large in comparison with kT) the meniscus may persist as the pressure is reduced below p_{1e}', equilibrium with the vapor being attained by the curvature of the surface, i.e., by the Kelvin effect, or what amounts to the same thing, by reduction of the hydrostatic pressure. Once this condition is attained, further decrease of the equilibrium pressure may cause greater curvature, thereby increasing the surface area and surface energy and hence tending to increase the permanence of the meniscus. Evidently, under such circumstances, if the surface tension is high we may reach a condition where the liquid is under a net negative pressure. When p_a is negative, p_c must be positive and accordingly the vapor pressure of the solid will be higher than it is when p_c is negative. Accordingly, although the thermodynamic potentials of two different adsorbate density states may be the same when p_c is either positive or negative, the thermodynamic potential of the solid will be higher when p_c is positive. Hence the system with p_a negative and p_c positive is thermodynamically unstable with respect to the system with p_a positive and p_c negative when both systems have the same adsorbate equilibrium pressure. Since the vapor pressure of the solid is assumed to be negligible, the permanence of the unstable state will be deter-

While the difference $p_a - p_{1e}$ is somewhat analogous to an osmotic pressure, strictly the osmotic pressure of the first component is $p_H - p_{1e}$ which in this case is practically zero.

mined by the magnitude of the activation energy involved in converting the one system into the other.

If p_a' and p_a are the pressures of adsorbates in equilibrium respectively with the relatively large gas pressures p' and p and the adsorbate states have been reached along the same path, we may write,

$$p_a' - p_a = \int_{u_1, u_s}^{u_1', u_s'} \frac{\rho_a}{u_1} dp_{1e},$$

or

$$\Delta p_a = \left|\frac{\rho_a}{u_1}\right| \Delta p. \tag{13}$$

Evidently while p_a may be greater or less than p, either negative or positive with respect to p, Δp_a must be of the same sign as Δp. If either u or ρ_a are not defined for a given value of p, the expression,

$$dp_a = \frac{\rho_a}{u} dp, \tag{14}$$

is essentially indeterminate for the given value of p. Thus at the saturation pressure where u is not defined, dp_a is not defined in terms of dp_s.

If we suppose the ideal porous solid to have pores of constant size, plausible equilibrium conditions as between the density, u, of a condensable vapor and the mean density, ρ_a, of adsorbate, would be as follows. Above the saturation pressure p_s, both u and ρ_a have the density of an incompressible liquid. In the equilibrium pressure region p_b to p_s, ρ_a has the liquid density, while the gas density corresponds to that of an ideal gas having the equilibrium pressure p_{1e} lying between p_b and p_s. Below p_b, ρ_a is considerably less than the liquid density and decreases with decreasing p_{1e}. The relations are illustrated in the following diagram.

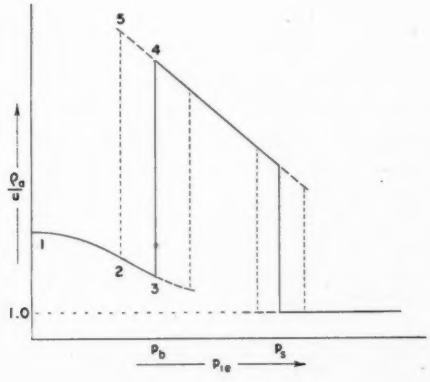

The solid line represents the path of the equilibrium values of ρ_a/u_1 as a function of p_{1e}. The broken lines represent metastable states that may be realized physically and are reversible with respect to changes along them. The dotted lines represent states of inherent instability and are not traversible. We calculate p_a for the point 5, by subtracting the area under the curve from 4 to 5 from the area under the curve from 1 to 3. However, we cannot calculate the value of p_a for the point 2 by this procedure, i.e., the dotted lines cannot be traversed when calculating mean values of ρ_a/u_1.

If we suppose the ideal porous solid to have a continuous distribution of pore sizes whose mean pore size falls within certain limits, the following phenomena should be observed. In the case of gases whose liquids have high surface tensions, as the gas pressure increases, the density of the fluid within the capillaries will increase in a manner depending on the specific forces concerned. As these forces may be supposed to fall off rapidly with the perpendicular distance from the solid surface, we might expect the mean density in small pores to increase more rapidly with pressure than it does in large pores. Accordingly, the number of pores having adsorbate whose density approaches that of the liquid density will increase as the gas pressure increases. The adsorbate will be in a state of compression and the solid in a state of tension, and accordingly the solid, if not quite rigid, will expand with increasing adsorption. If in the expanded state an appreciable number of pores are liquid filled and the surface energy per pore is large in comparison with kT, the menisci may persist when the pressure is reduced. The curvature of menisci will change from the original curvature becoming more convex toward the liquid, thereby reducing the hydrostatic pressure in these pores. The net pressure of adsorbate will thus be reduced while the net pressure of the solid is increased. In the case of some of the larger capillaries, if the surface forces, pore radii, and wetting angles are such that the maximum possible curvatures are insufficient to reduce the vapor pressures to the equilibrium value, the fluids in these pores will evaporate and return to their previous condition, altered somewhat by the altered net state of tension or pressure of the solid. If the pressure is again increased, the system may or may not return to the original condition depending on the permanence of the "configuration" of the solid resulting from the tensions and pressures in the various pores. Evidently if the solid is exposed to such a gas pressure that all of the pores are liquid filled and the pressure is reduced, if the pore sizes are all of nearly the same size and the menisci persist, practically the whole of the adsorbate may reach a condition where it is under a very considerable state of tension. The solid under these conditions will be in a state of compression and, if not quite rigid, may contract to a volume considerably less than its volume when the gas pressure is zero. The mean density of the adsorbate in this case may be much higher than that obtained at the same gas pressures when approached from zero pressures, i.e., we get marked hysteresis. It may be remarked that if a vapor is very strongly adsorbed and especially if the fields within capillaries are almost uniform, practically

the whole of the micropore volume may be filled with liquid adsorbate whose vapor pressure is considerably less than that of the normal liquid with any surface curvature consistent with the pore structure. Again, if the surface tension is small or if the mean pore size is small so that the surface free energy of each meniscus is small compared with kT, the surface will be labile and have no permanence, the situation resembling somewhat that which prevails when a liquid approaches its critical temperature and opalescence appears. In either of these two cases hysteresis due to capillary condensation is not to be expected. While hysteresis is probably usually associated with phase changes, hysteresis is not, of course, necessarily due to "bottleneck" structures in any literal sense.

Evidently, the above simple picture is consistent with the adsorption behavior of our carbon rods. At higher relative pressures where adsorption is considerable, the various expansions and contractions observed by McIntosh (7) for similar carbon rods can be estimated fairly accurately from the values of $|\overline{\rho_a/u}|$ taken from the relevant adsorption and desorption isotherms.* Accordingly, we feel that the treatment of the adsorbate as the same fluid as the adsorbable gas, but having a different hydrodynamic pressure, is essentially correct in regions where considerable adsorption occurs.†

It may be felt that the foregoing discussion is not germane to flow problems. However, it is absolutely necessary to establish the fact that the adsorbate may be considered as the same fluid as the equilibrium gas in the sense that the adsorbate has the properties of the equilibrium gas when the gas is compressed to the adsorbate density, i.e., to establish the fact that the adsorbate behaves in a manner analogous to that of a condensible gas in a gravitational field. Otherwise there would be no justification whatever for the relations put forward above, which are at best only approximations. If we know that the adsorbate and adsorbable gas may be regarded as two "phases" of a single component, the condition for equilibrium at constant temperature can be written at once, $dp_a/\rho_a = dp_1/u_1$, and hence we can obtain Equations 13 and 14 immediately. It is thought that in the above discussion some points of interest are brought out which are usually omitted in published discussions on this subject.

If a long, activated carbon rod is exposed at its two ends to the different gas pressures p_1 and p_2 and we suppose that the rate of flow through the carbon is slow compared with the rate of adsorption and desorption, we may suppose the two ends of the rod to be very nearly in equilibrium with the corresponding gas pressures. If the difference between the gas pressures is

Where considerable hysteresis is observed, probably $|\overline{\rho_a/u}|$ is better estimated along the hysteresis scanning loops.

†*At low relative pressures where the adsorbate can hardly be regarded as a continuous fluid distinct from the adsorbent, the above discussion can have very little validity. Even if the adsorbate can still be regarded as a one component fluid distinct from the adsorbent, the low surface coverage associated with very low equilibrium pressures may give rise to isolated compressive forces. The action of isolated nonisotropic compressive forces within the pores of the carbon may give rise to either an increase or a decrease in the length of the sample. Hence the small length changes associated with adsorption at low pressures can not be correlated with adsorption data with any reliability.*

Δp, the difference between the corresponding hydrodynamic adsorbate pressures, Δp_a, will be given approximately by,

$$\Delta p_a = \left|\overline{\frac{\rho_a}{u}}\right| \Delta p.$$

If ρ_a is at all comparable with the liquid density and u is the gas density at low gas pressures, Δp_a may exceed Δp by very large factors. If the carbon exhibits hysteresis toward the gas, it will be necessary to know that the equilibrium states along the rod and at the two ends correspond to desorption or adsorption states. While probably neither the adsorption nor desorption branch corresponds to the true equilibrium path, the adsorption branch should be close enough for most practical purposes. Evidently surface forces may give rise to very large forces tending to push (adsorption) or pull (extreme cases of desorption) the adsorbate through the porous system when the system is exposed to different adsorbable gas pressures at each end.

HYDRODYNAMIC CONSIDERATIONS

If a fluid is flowing very slowly through a long narrow cylindrical pipe under steady flow and isothermal conditions, we may assume that the fluid is in a state of thermodynamic equilibrium throughout any cross section perpendicular to the direction of flow or to the axis of the pipe, i.e., we may assume laminar flow. We shall assume that velocity contours are geometrically similar to that of the pipe. For simplicity the pipe is assumed circular. We consider the forces acting on an elementary fluid disk whose center lies on the axis of the circular pipe (*cf.* Part I, Page 365).

If the area of the disk is A and the mean fluid pressure difference on the two faces of the disk is δp_a, the total force acting on the disk tending to move it toward $+ z$ is $A\overline{\delta p_a}$. Then balancing forces acting on the disk, we have,*

$$A\overline{\delta p_a} = \eta \delta z S \overline{G},$$

or for the forces acting on an elementary annulus of radius, x,

$$\frac{\partial A}{\partial x}\delta x\, \delta p_a(x) = \frac{\partial}{\partial x}(\eta \delta z S \overline{G})\delta x. \tag{15}$$

We shall use as a measure of the pressure difference across the fluid disk the pressure difference between the gases with which the two faces of the disk would be in thermodynamic equilibrium through semipermeable membranes. Since the fluid is assumed to be in a state of thermodynamic equilibrium across a section, the equilibrium gas pressure difference, δp, will be constant in a given section, i.e., δp will be independent of x.

If $\rho(x)$ is the density of the fluid in any annulus of radius x, and u is the equilibrium density of the reference gas beyond the influence of any possible surface forces, then,

*S *is the perimeter of the elementary disk,* $S\delta z$ *the surface of shear, and* $\overline{G}$ *the mean value of the velocity gradient as in Part I.*

$$\delta p_a = \frac{\rho(x)}{u}\delta p \tag{16}$$

where δp_a is the pressure difference across a fluid annulus whose density is $\rho(x)$ and δp is the corresponding pressure difference of the reference gas, whose density is u.

If we know the weight of fluid contained within the pipe for various values of u or p (i.e., if we know the adsorption isotherm) we have a direct measure of ρ_a, the mean density of the fluid. ρ_a will be given by,

$$\rho_a = \frac{2}{r^2}\int_0^r \rho(x)x\,dx, \qquad 0 \leqslant x \leqslant r,$$

where r is the radius of the pipe. Hence $\rho(x)$ must be consistent with ρ_a. However, even if we know ρ_a, without a knowledge of $\rho(x)$ we cannot calculate the velocity distribution in a cross section and cannot calculate the flow rate.

From physical considerations it is evident that there will be a considerable number of cases where $\rho(x)$ may be represented by functions of the following type,

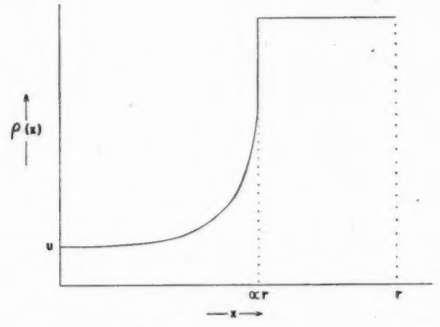

$$\begin{aligned} \rho_1(x) &= u + Cx^n, & 0 \leqslant x \leqslant \alpha r, \quad \eta = \eta_g, \\ \rho_2(x) &= \rho_l, & \alpha r < x \leqslant r, \quad \eta = \eta_l, \end{aligned} \tag{17}$$

where the fluid is a gas in the interval 0 to αr and its viscosity is the gas viscosity η_g and is independent of the density $\rho_1(x)$, while in the interval αr to r the fluid is a liquid having the corresponding liquid density ρ_l and viscosity η_l which are assumed independent of x and p. The parameters C, n, and α are independent of x but may be functions of p (or u) and r. The parameters, of course, vary with the kind of gas and nature of the capillary surface.

From Equations 15, 16, and 17 we can obtain expressions for the velocity of the annulus as a function of (x).

In the region 0 to αr,

$$V_1(x) = \frac{x^2}{4\eta_g}p_z + \frac{Cx^{n+2}}{\eta_g(n+2)^2u}p_z + I_1$$

and in the region ar to r,

$$V_2(x) = \frac{x^2}{4\eta_l}\frac{\rho_a}{u}p_z + I_2$$

where p_z is written for $\delta p/\delta z$ and I_1 and I_2 are integrating constants.

The experimental evidence suggests that the gas slip velocity is almost the same on any high-density surface; accordingly, the velocity of the annulus at $x = ar$ will be very nearly equal to the normal gas slip velocity plus the velocity of the liquid layer at this value of x. While we can only form a vague notion as to the liquid slip velocity, it should be estimated and included. The constants I_1 and I_2 can then be determined in terms of the parameters and accordingly the flow rate also expressed in terms of the parameters. The flow rate in mass units will be given by,

$$Q_m = 2\pi\int_0^{ar} V_1(x)\rho_1(x)x\,dx + 2\pi\rho_l\int_{ar}^{r} V_2(x)x\,dx.$$

Representing the integral by $-I(p,r)\,dp/dz$ we can write,

$$Q_m = -I(p,r)\frac{dp}{dz},$$

and since in the steady flow Q_m must be constant for every section, we can integrate over the intervals $p_1 \leqslant p \leqslant p_2$, $0 \leqslant z \leqslant L$, and obtain,

$$Q_m = \overline{I(p,r)}\,\frac{p_1 - p_2}{L},$$

or, expressing the flow in K units,

$$K = \frac{RT}{M}\,\frac{\overline{I(p,r)}}{L}.$$

For N cylinders or capillaries of different radii and lengths in a parallel arrangement we thus get,

$$K = \frac{RT}{M}\sum_N \frac{\overline{I_i(p,r)}}{L_i}$$

where K is the rate of flow in K units through the N straight capillaries whose ends are in equilibrium with the gas pressures p_1 and p_2.

The mean density which may be assumed known from isotherm data will be given by

$$\rho_a = \frac{1}{\sum_N r_i^2 L_i}\sum_N\left[a^2\left(u + \frac{2ca^n r^n}{n+2}\right) + \rho_l(1 - a^2)\right]r_i^2 L_i.$$

In the general case, C, n, and a must be regarded as functions of both the radius and the pressure and the only condition which they must meet is that they yield a value of the mean density ρ_a as a function of u or p which is consistent with isotherm data. Accordingly, the summations may yield a

variety of more or less arbitrary complex expressions. Even if the capillary radii and lengths are all the same, the expression resulting from the integral is still highly arbitrary and can give widely different flow rates for given isotherm data (among other reasons because of the relatively large differences between liquid and gas viscosities).

There are two cases where we can considerably simplify the expressions and obtain less arbitrary flow formulae which should be applicable to single capillaries or to systems of capillaries of constant radius.

Case I: First we may consider the reference gas to be very dilute and far above its critical temperature so that we may assume that no liquid forms. In this case $a = 1$ and we get the following relations:

The mean density* will be given by,

$$\rho_a = u + \frac{2Cr^n}{n+2},$$

and the flow rate through a single capillary by,

$$Q_m = -\frac{\pi r^4}{\eta_g} p_z \left[\frac{u}{8} + \frac{\rho_a - u}{n+4} + \frac{(\rho_a - u)^2}{4(n+2)u}\right] - \pi r^3 p_z \sqrt{\frac{\pi M}{2RT}} \cdot \frac{\rho_a^2}{(n+2)\rho_a u - nu^2},$$

which for $\rho_a \gg u$, neglecting small terms yields,

$$Q_m = -\frac{\pi r^4}{4(n+2)\eta_g} \frac{\rho_a^2}{u} p_z - \frac{\pi r^3}{n+2} \sqrt{\frac{\pi M}{2RT}} \frac{\rho_a}{u} p_z. \tag{18}$$

Case II: Secondly, we consider a case where the fluid is considerably below its critical temperature and where the vapor pressure of the liquid is relatively small so that we may neglect any variation in gas density and thus consider the fluid to be essentially a liquid film, i.e., we put $C = 0$. Under these circumstances,

$$\rho_a = ua^2 + \rho_l(1 - a^2), \quad \text{or} \quad a^2 = \frac{\rho_l - \rho_a}{\rho_l - u}$$

and the flow rate in mass units through a single capillary becomes,

$$Q_m = -\frac{\pi r^4}{8} p_z \left\{\frac{u}{\eta_g}\left(a^4 + \frac{4\xi_1 a^3}{r}\right) + \frac{2\rho_l}{\eta_l} a^2(1 - a^2) + \frac{4\rho_l}{\eta_l}\frac{\xi_2 a^2}{r} \cdots \right.$$
$$\left. \cdots + \frac{1}{\eta_l}\frac{\rho_l^2}{u}(1 - a^2)^2 + \frac{4\xi_2}{\eta_l r}\frac{\rho_l^2}{u}(1 - a^2)\right\},$$

where ξ_1 and ξ_2 are the coefficients of slip of gas and liquid respectively. When $\rho_a \gg u$, $\rho_l \gg u$, and $\rho_a \to \rho_l$ after eliminating a and neglecting the small liquid slip we get the very simple expression

**While over large pressure ranges (i.e., large ranges in values of u) n is almost certainly pressure dependent, over comparatively small ranges we may take n as practically independent of pressure. Since ρ_a is always much greater than u for adsorbable gases, we can obtain an expression for the maximum density, $\rho(r)$, in terms of the mean density, namely, $\rho(r) \to \frac{1}{2}(n+2)\rho_a$. This relation imposes upper limits on plausible values of n in various pressure regions. Thus at lower pressures n can hardly exceed 10 and at higher relative pressures n is probably of the order of unity or less.*

$$Q_m = -\frac{\pi r^4}{8\eta_l}\frac{\rho_a^2}{u}p_z . \tag{19}$$

If either one of these ideal cases* may be considered as descriptive of the conditions which prevail in our charcoal rods during a steady state of flow through the micropore system, the second case would appear to be the more probable since in the higher relative pressure regions the fluid in the micropores must be essentially liquid. The Langmuir and B.E.T. theories of multilayer adsorption as well as the capillary condensation theory suggest that any laminar or viscous flow of a fluid adsorbate film should be controlled by a density and viscosity very nearly those of the normal liquid. Accordingly, Equation 19 rather than Equation 18 seems to be indicated, at least in the regions where considerable adsorption occurs.†

In order to make any further progress it is essential to have a great deal of information concerning the micropore structure from which to construct a model pore system. It is especially necessary to have information concerning the distribution of pore sizes since in the case of multilayer adsorption the mean density per pore is almost certainly a function of the radius, while in capillary condensation the fraction of the pores filled is a function of the radius. In the case of our carbon rods the evidence indicates that the pores of the micropore system are of nearly constant size. Unfortunately, however, we are not too sure of what this size is, since, as pointed out by Emmett (3), the apparent diameters of the pores as measured by the water desorption isotherm depend on the assumed shape, about which we have little or no information.

*Since η_g is of the order of $10^{-2}.\eta_l$ and, in the higher relative pressure regions, n is of the order of unity, the Poiseuille flow rate alone according to Equation 18 is roughly a hundredfold the total flow rate according to Equation 19.

†We have seen (page 391) that in the case of long narrow circular capillaries, the ratio of the flow rates of liquids of low vapor pressure to the flow rates of their saturated vapor could be represented by Equation 5, namely,

$$\frac{K_l}{K_g} \rightarrow r(10^5 \text{ to } 10^6) + \gamma.$$

If we suppose the vapor pressure reduced at each end of the capillary and equilibrium with the vapor at the two ends maintained by the curvatures of surfaces of tension, i.e., by negative liquid pressures, then in the case of very long capillaries where the flow rate does not disturb the equilibrium and where the dimensions of the capillary are not too small compared with molecular diameters so that viscous flow can take place, we must have,

$$\frac{K_l}{K_g} \rightarrow r(10^5 \text{ to } 10^6)\left|\overline{\frac{\rho_a^2}{u}}\right| + \gamma\left|\overline{\frac{\rho_a}{u}}\right| , \tag{5(a)}$$

where K_l represents the liquid flow rate under conditions of capillary condensation and K_g the corresponding effusive gas flow in the absence of appreciable condensation or adsorption. Evidently Equation 5 may be regarded as a special case of Equation 5a. Taking ρ_a as of the order of unity we can write Equation 5a in the form,

$$\frac{K_l}{K_g} \rightarrow r\,(10^{10} \text{ to } 10^{12})\left|\overline{\frac{1}{p_m}}\right| + \gamma\,(10^5 \text{ to } 10^6)\left|\overline{\frac{1}{p_m}}\right| ,$$

where p_m is the vapor equilibrium pressure in mm. Hg.

Evidently under these idealized conditions surface forces are capable of increasing flow rates of condensable vapors a millionfold or more without any regard for what is properly surface diffusion. However, above the saturation pressure when the fluid within, as well as outside of, the capillary is an almost incompressible liquid, surface forces cannot increase flow rates appreciably under the conditions postulated.

Further, we have little or no information as to whether the micropore system should be regarded as an interstitial structure or as a system of long capillary passages. In the absence of information to the contrary, we adopt the model commonly used in these problems, namely, a system of round nonintersecting straight capillaries of constant radius; one-third of them parallel to, and two-thirds of them perpendicular to the pressure gradient; all the capillaries of lengths corresponding to the dimensions of the sample. Regardless of its merits, this ideal pore system, because of its familiarity, is perhaps most suitable for use in conjunction with a proposed flow mechanism.*

On the basis of this model the flow rate through a thin section of micropore system may be written,

$$Q_m = -\frac{N\pi r^4}{8\eta_l}\frac{\rho_a^2}{u}\frac{dp}{dz} = -\frac{D^2 V_a'}{96\eta_l}\frac{\rho_a^2}{u}\frac{dp}{dz},$$

where N is the number of pores per unit area, V_a' is the void volume per cubic centimeter of micropore system, D is the pore diameter. For a sample of micropore system of unit length and area, $V_a' = 3N\pi r^2$.

Since as we have seen (Part I, page 360) we may regard the pressure drop as constant across any thin section of the porous body normal to the pressure gradient, the flow through a system of micropores and macropores will be the sum of the flows through each system, more or less independently. Assuming that the gas density in the macropore system is not appreciably influenced by adsorption effects, we can write for the total flow rate through a section of unit area containing both macropores and micropores the following,

$$Q_m = -A' p\frac{dp}{dz} - B'\frac{dp}{dz} - \frac{f'(a)D^2 V_a'}{96\eta_l}\frac{\rho_a^2}{u}\frac{dp}{dz},$$

where A' and B' refer to macropore system and are to be calculated as indicated in Part II; $f'(a)$ is the so-called shape factor, a factor due to departures of the actual micropore structure from the assumed model. Since Q_m is constant throughout the sample in the steady state of flow, we can integrate and express the flow rate in K units for a sample of area O and length L. Thus,

$$K = \frac{A}{\eta_g}\bar{p}_m + \frac{B}{\sqrt{M}} + \frac{O}{L}f(a)\frac{RT}{M}\frac{D^2 V_a}{96\eta_l}\left|\overline{\frac{\rho_a^2}{u}}\right|_{\Delta p}$$

where V_a is now the void volume of the micropore system per cubic centimeter of the whole sample of both micropores and macropores, and $f(a)$ is a new shape factor involving the mean pore length of the micropores in the whole assembly. A and B are to be calculated as previously indicated. Since we

**If the flow mechanism can be established as a laminar viscous flow, then with the assumption that velocity and density contours are geometrically similar to that of the "average pore" we could treat the micropore system in terms of stochastic variables along the lines employed previously (Part II) in treating the macropore system. We could thus extend the treatment to model pore systems of a variety of arrangements and cross-sectional shapes.*

have assumed that the micropore radius may be regarded as constant for this type of activated carbon, ρ_a is independent of r, $\Sigma r^4 N(r)$ is independent of u, and $\rho_a = X\rho'/V_a$, where X is the weight adsorbed per gram of sample and ρ' is the apparent or bulk density of the whole assembly of carbon and void space (0.707). Assuming the gas laws to hold for the equilibrium gas, $u = pcM/RT$, where the symbols are as previously indicated. Hence, we obtain for the flow rate in K units through the sample of area O and length L between the pressures, p_1 and p_2,

$$K = \frac{A}{\eta_g}\bar{p}_m + \frac{B}{\sqrt{M}} + \frac{O}{L}f(a)\frac{D^2}{96\eta_l}\left(\frac{RT}{M}\right)^2\frac{(\rho')^2}{cV_a}\left|\overline{\frac{X^2}{p_m}}\right|_{\Delta p}, \tag{20}$$

where $\left|\overline{X^2/p_m}\right|_{\Delta p}$ is the mean value, over the pressure interval, p_1 to p_2, of the square of the weight adsorbed per gram of sample, divided by the corresponding equilibrium pressure in mm. of Hg.

In the case of our samples taking the value of $\bar{D}$ as 1.2×10^{-7}, as indicated by Juhola's data* (3, 5), together with a bulk density, ρ', of 0.71 and a micropore void volume, V_a, of 0.38 cc. per cc. of carbon and $T = 308°$K., we get for the flow rate per minute,

$$K = \frac{A}{\eta_g}\bar{p}_m + \frac{B}{\sqrt{M}} + 6.6 \times 10^2\frac{f(a)}{M^2\eta_l}\left|\overline{\frac{X^2}{p_m}}\right|_{\Delta p}.$$

It is found that with $f(a)$ varying between about 0.3 and 1.5 for the various gases, all of the flow data can be fitted fairly well. If the difference between the observed total flow and the calculated gas flow through the macropore system is represented by ΔK, then taking $f(a)$ as unity, ΔK is given by,

$$\Delta K = 6.6 \times 10^2\frac{1}{M^2\eta_l}\left|\overline{\frac{X^2}{p_m}}\right|_{\Delta p}. \tag{21}$$

The solid lines in Figs. 1 to 5 are calculated from Equation 21; the dotted lines represent the observed total flow minus the calculated flow through the macropore system. In the case of water under desorption (capillary condensation) conditions, the calculations were made directly from the desorption branch of the hysteresis loop rather than from "reversible" scanning loops. It may be remarked that in the case of ethyl chloride, the gas viscosity used is almost certainly too high, consequently the "apparent" observed micropore flow is probably considerably less at higher pressures than shown by the dotted line.

While Equation 20 does not fit the data as well as Equation 6 and is not perhaps as convenient arithmetically, it can, of course, be made the basis of a much less arbitrary empirical equation that will fit the data. It is to be borne

**If Equation 20 is used to calculate $\overline{D}$ from the flow data for the various adsorbable gases, we get somewhat different values, all of which, however, are close to 1.2×10^{-7} cm. It may be remarked that the apparent value of $\overline{D}$ in round capillaries of constant radius throughout a given length will be much the same toward the Kelvin equation as toward the flow equation. $\bar{D}$ will probably be somewhat smaller than the actual diameter, very strongly adsorbed molecules behaving more as part of the wall than as part of the fluid.*

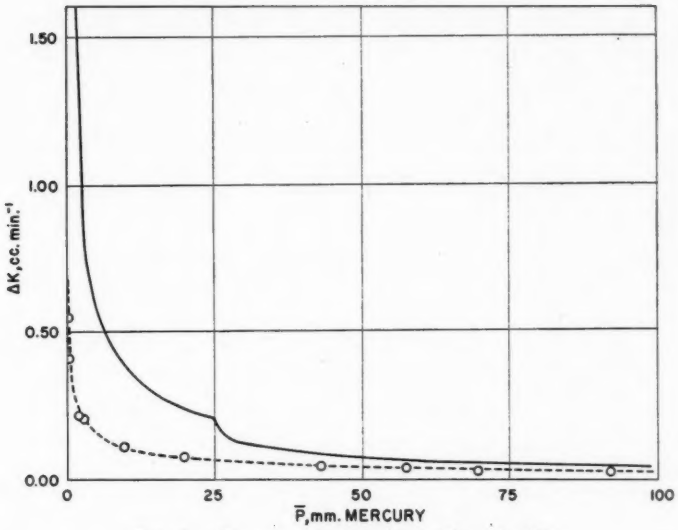

FIG. 1. Benzene micropore flow. Plug No. 18.

NOTE:

In Figs. 1 to 5 inclusive, the circles represent the observed flow rates less the gaseous flow rates calculated from nitrogen permeability. The broken lines are curves drawn through the circles. The unbroken lines are calculated from Equation 21. In Fig. 5 the solid and open circles refer to flow rates under desorption and adsorption conditions, respectively, and are to be compared with the upper and lower unbroken calculated curves, respectively. The values of the physical constants used in the calculations are the same as those used previously and are given in Table II, Part I of this series of papers.

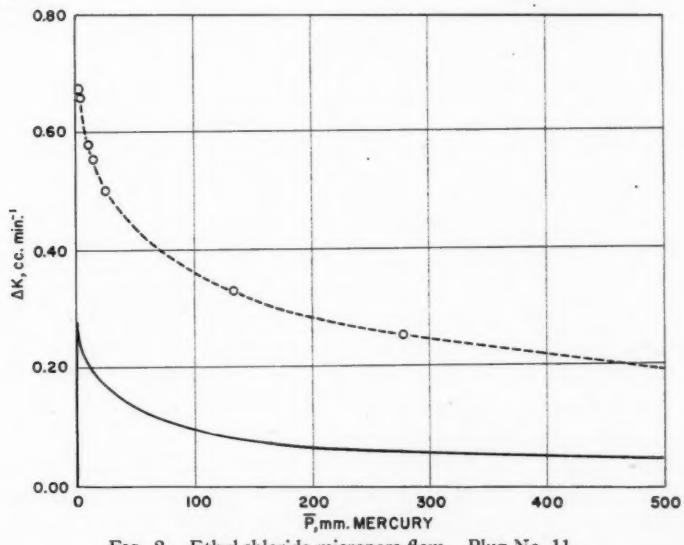

FIG. 2. Ethyl chloride micropore flow. Plug No. 11.

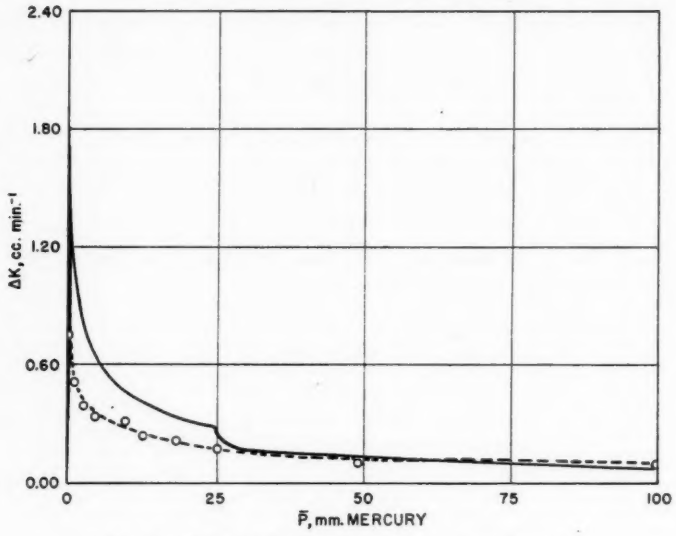

FIG. 3. Diethyl ether micropore flow. Plug No. 18.

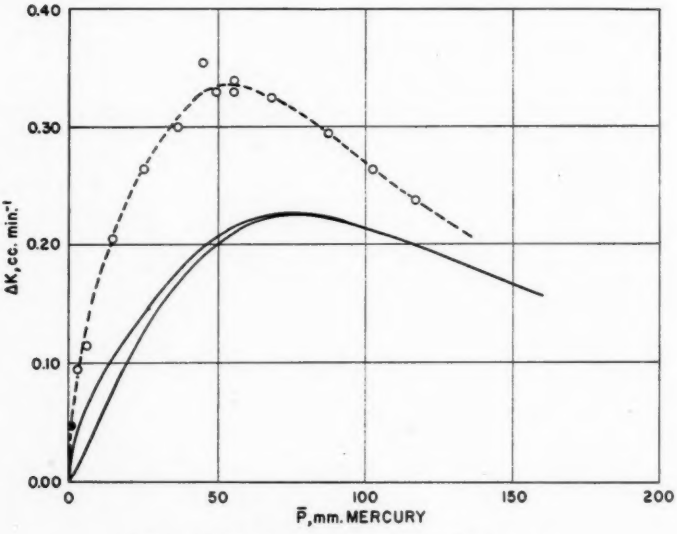

FIG. 4. Methanol micropore flow. Plug No. 11.

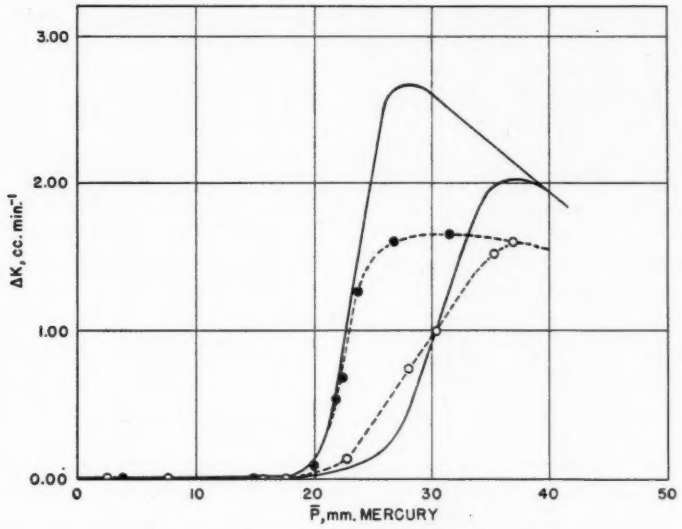

FIG. 5. Water micropore flow. Plug No. 11.

in mind that the observed flow is a combination of the flow through the micropore and macropore systems. Any errors or inconsistencies in adsorption data, vapor or liquid viscosities, etc., will have a considerable influence on the apparent agreement between observed and calculated values of ΔK. It is considered that the agreement between the observed and calculated results is as close as could be expected even if Equation 21 were exact. Of course, neither Equation 21 nor Equation 20 can be exact in any case since a number of inadmissible simplifying assumptions have been made in their derivation. As far as these equations are concerned, obvious inconsistencies are involved in the summation over the pore radii. While Equation 19 describes a flow through a single pore which might be approached by real pores under certain conditions, Equation 20 describes a condition that can only be approached when micropore radii are practically constant, i.e., when the actual pore system behaves like the model. Further, it must be emphasized that the fact that the micropore "shape factor" is nearly unity must be regarded as largely fortuitous. Physically plausible model pore systems can be constructed which are consistent with the micropore void volume and Juhola's data, but which require that $f(a)$ be greater or less than unity by large factors, those greater than unity being perhaps the more plausible.

However, in spite of its shortcomings, Equation 20 is consistent with a good many reasonably well-established facts concerning such carbon rods. It gives a fairly reliable correlation in absolute units between the flow rates of a variety of fluids, the adsorptive properties of the carbon, and its coarse and fine structures. All of the parameters and variables except those related to structures are directly measurable quantities. The terms describing the

structure, especially those describing the macropore system, are not by any means entirely arbitrary. Where the form of the frequency distribution of macropore diameters is known and where the micropore diameters are nearly constant, Equation 20 yields values of the mean pore diameters of both macropore and micropore systems which are entirely consistent with those obtained by independent methods. Accordingly, we feel that the ideas underlying the derivation of Equation 20 have some validity. While there are a number of more or less obvious corrections which must be introduced if a description of the micropore flow rate of any accuracy is required, the available data does not warrant anything better than a rough qualitative description of the main factors involved.

CONCLUSION

While we cannot separate completely the flows through the micropore and macropore systems, nor in the case of the micropore flow, can we distinguish clearly between a viscous flow of compressed gases, a flow of liquid films, or a combination of both, our results indicate that contributions from purely diffusive types of flow are small under our experimental conditions. In regions where considerable adsorption occurs and either multilayer adsorption or capillary condensation is indicated, the evidence suggests that the rate-controlling mechanism of flow through the micropore system of our carbon rods is a laminar viscous flow of liquid films. Of course, it is not intended to imply that surface diffusion phenomena do not occur. Obviously, processes of this type must occur and in extreme cases must be rate controlling.

REFERENCES

1. BABBITT, J. D. Can. J. Research, A, 28: 449. 1950.
2. CARMAN, P. C. Proc. Roy. Soc. (London), A, 203: 55. 1950.
3. EMMETT, P. H. Chem. Rev. 43: 69. 1948.
4. FOWLER, R. H. and GUGGENHEIM, E. A. Statistical thermodynamics. The University Press, Cambridge. 1939. Chap. X.
5. JUHOLA, A. J. Division 10, NDRC Formal Report, June, 1945.
6. KENNARD, E. H. Kinetic theory of gases. McGraw-Hill Book Co., Inc., New York. 1938.
7. MCINTOSH, R. L., HAINES, R. S., and BENSON, G. C. J. Chem. Phys. 15: 17. 1947.
8. TOMLINSON, R. H. and FLOOD, E. A. Can. J. Research, B, 26: 38. 1948.

1-INDOLEACETIC ACID[1]

By W. S. Smith[2] and R. Y. Moir[3]

ABSTRACT

1-Indoleacetic acid, 3-methyl-1-indoleacetic acid, and several of their derivatives were formed from phenylhydrazineacetic ester, and their structures were determined in three different ways. Several of the new compounds exhibited plant growth regulating activity.

In this paper it is shown that 1-indoleacetic acid (I) and some of its derivatives may be formed from asymmetrical phenylhydrazineacetic ester hydrochloride (II) by conventional methods, and that some of these derivatives exhibit plant growth regulating activity to an interesting degree. The problem was suggested to us several years ago by Dr. R. H. Manske.

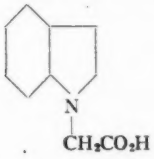

I

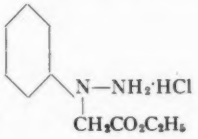

II

Phenylhydrazineacetic ester hydrochloride (II) was made from phenylglycine by the method of Harries (6) and also from phenylhydrazine and chloroacetic acid by the method of Busch (2). The former method gave a product of unambiguous structure, but the latter method was much more convenient. Two new demonstrations of the identity of the products made by the two methods are described in the experimental part and are desirable because of the previous confusion regarding the structure of the substance made by the second method (2, 6, 14).

Condensation of phenylhydrazineacetic ester hydrochloride (II) with ethyl pyruvate in alcoholic hydrogen chloride gave excellent yields of the diethyl ester of 2-carboxy-1-indoleacetic acid (III*a*). The ester was easily saponified to give the free acid (III*b*), which readily formed the anhydride, the acid amide (IV*a*?), and the half ester (IV*b*). Decarboxylations of the half esters of 2-carboxy-3-indoleacetic acids by heating them either alone or in quinoline in the presence of a copper chromium oxide catalyst have been performed by King and L'Ecuyer (10), by Tanaka (16), and by Findlay and Dougherty (4), but large amounts of tar were formed when their methods were applied to the half ester IV*b*. It was thought that dilution of the reaction mixture with

[1] *Manuscript received January 9, 1952.*

Joint contribution from the Research Laboratories of the Dominion Rubber Company and from the Department of Chemistry of Queen's University. The greater part of the material in this paper is taken from a thesis written by W. S. Smith in August 1951, in partial fulfillment of the requirements for the degree of Master of Arts.

[2] *Present address: Fabrikoid Division, Canadian Industries Ltd., Toronto, Ont.*

[3] *Formerly at the Research Laboratories, Dominion Rubber Company, Ltd., Guelph, Ont. Present address: Department of Chemistry, Queen's University, Kingston, Ont.*

large amounts of quinoline should favor the decarboxylation in competition with the formation of tar, since the former reaction should be unimolecular and the latter at least bimolecular in IV*b*. Dilution did suppress the formation of tar but another interesting complication arose. The quinoline contained small amounts of aniline and in the decarboxylations carried out in large volumes of quinoline, some anilide of 1-indoleacetic acid (V*b*) was formed as well as the expected ester (V*a*). The formation of the anilide was not un-

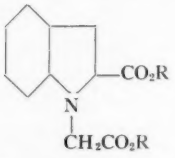

III*a*: R = C_2H_5
III*b*: R = H

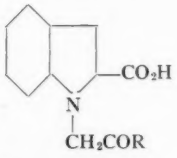

IV*a*: R = NH_2
IV*b*: R = OC_2H_5

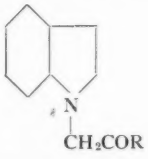

V*a*: R = OC_2H_5
V*b*: R = NHPh

welcome since it was a highly crystalline and stable derivative of the rather unstable free acid (I) and since it proved to be highly active as a plant growth regulator. Hydrolysis of either the ester (V*a*) or the anilide (V*b*) gave the desired 1-indoleacetic acid (I) as small, shining needles of melting point 179°C. It was a rather unstable substance, difficult to purify.

Phenylhydrazineacetic ester hydrochloride (II) and the methyl ester of α-ketobutyric acid were smoothly converted in ethanolic hydrogen chloride to the *diethyl* ester of 2-carboxy-3-methyl-1-indoleacetic acid (VI*a*), which

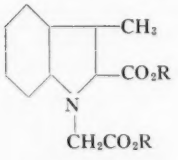

VI*a*: R = C_2H_5
VI*b*: R = H

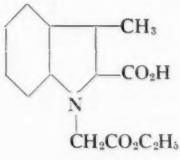

VII

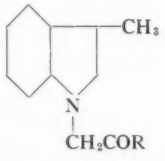

VIII*a*: R = OC_2H_5
VIII*b*: R = NHPh
VIII*c*: R = OH

was readily hydrolyzed to give the free acid (VI*b*). Conversion of the latter to its half ester (VII) occurred easily, and when VII was heated in quinoline with copper chromium oxide, a mixture of the ethyl ester (VIII*a*) and the anilide (VIII*b*) of 3-methyl-1-indoleacetic acid was formed. Tar formation during the decarboxylation was much less than in the decarboxylation of IV*b*, as was expected since the reactive 3-position was occupied in VII but not in IV*b*. Hydrolysis of the ester (VIII*a*) gave the free 3-methyl-1-indoleacetic acid as white crystals of melting point 179°C., somewhat more stable than those of 1-indoleacetic acid.

The 3-methyl-1-indoleacetic acid (VIII*c*) prepared in this way proved to be identical with that made by Jackson and Manske (8) from 1,3-indolediacetic acid (IX), a rather conclusive proof of the structures suggested in the present

paper for the monocarboxylic acids and their derivatives and for the dicar-

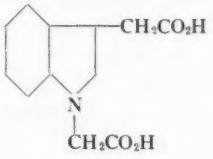

IX

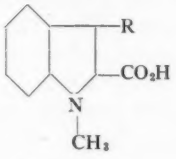

X*a*: R = H
X*b*: R = CH_3

boxylic acids and their diethyl esters. These structures were confirmed in two other ways. Decarboxylation of the dicarboxylic acids III*b* and VI*b* could lead either to the acids I and VIII*c*, or to the acids X*a* and X*b*, respectively, depending on which carboxyl group was lost. The acids X*a* (5) and X*b* (9) are known; both melt at 212°C. rather than at 179°C. as do both of the monocarboxylic acids obtained in the present work, so that structures I and VIII*c* were confirmed. The fact that the compounds thought to be III*b*, IV*b*, VI*a*, VI*b*, and VII gave negative tests with Ehrlich's reagent, while the compounds thought to be I, V*a*, V*b*, VIII*a*, VIII*b*, and VIII*c* all gave strongly positive tests with the reagent also confirmed the structures suggested for them, since the intensified color given by the second set of compounds was evidence that they had lost a carboxyl group in the 2-position (4). The structures of the half esters of the dicarboxylic acids were given as IV*b* and VII because of their decarboxylation to V*a* and VIII*a* respectively. This method of proof has been accepted by several authors (4, 10, 16) but is perhaps not absolutely conclusive because of the drastic conditions used in the decarboxylations. Finally, the structure of the half amide of 2-carboxy-1-indoleacetic acid was thought to be IV*a* because of its analogy to the half esters (IV*b* and VII) and to the anilides (V*b* and VIII*b*).

Some of the new indole derivatives were compared with 3-indoleacetic acid in their ability to produce cell elongation in young tomato plants, as suggested by Zimmerman (17). Our tests were not sufficiently accurate or extensive to make quantitative comparisons advisable, but they did establish the fact that some of the compounds, notably the anilide of 1-indoleacetic acid, were highly active as plant growth regulators. This observation was of considerable interest because of the geometrical similarity of the compounds to the very active 3-indoleacetic acid.

EXPERIMENTAL

Melting points are corrected unless otherwise stated.

asymm-Phenylhydrazineacetic Ester Hydrochloride

(*a*) *By Harries' Method* (6)

N-phenylglycine (12) was esterified in 50% yield with ethanol and hydrogen chloride (15) or in 64% yield with ethanol and sulphuric acid, and the ester was quantitatively converted to its N-nitroso derivative as described by

Harries (6). Less zinc dust and alcohol (7) than suggested by Harries were used in the reduction of the nitroso compound, but our yields were much lower than his. The crude phenylhydrazineacetic ester was obtained from the reduction as a red syrup; attempts to purify it by Harries' method failed, but a method like that of Busch (2) succeeded. The red syrup was dissolved in absolute ethanol and the solution was saturated with dry hydrogen chloride. After the mixture had been thoroughly chilled, the slightly pink needles which formed were recovered, washed with alcohol and with ether, and dried first in the air and then *in vacuo* over sulphuric acid. The yield was 18% and the melting point of the crystals was 194.8-195.7°C. with decomposition. In other experiments one of us obtained yields of 20% and 23%. Harries reported a yield of 55%, and a melting point of 195-196°C.

(*b*) *By Busch's Method* (2)

Crude *asymm*-phenylhydrazineacetic acid was made according to Busch's directions in a yield of 83%, but the product soon turned to a gum and its subsequent reactions failed. In another run, the crude acid was *immediately* recrystallized from 60% alcohol to give a heavy crop of light yellow needles in a yield of 46%. This product was stable. The once-recrystallized acid (37.7 gm.) was suspended in absolute ethanol (240 cc.), the mixture was thoroughly saturated with hydrogen chloride, and then heated under reflux for 30 min. Yellow needles separated from the cooled reaction mixture and were recovered, washed with ethanol, and rigorously dried; yield 33.4 gm. or 64%, m.p. 192.6-194.6°C. with decomposition, mixed m.p. with the ester hydrochloride prepared by Harries' method 193.0-195.1°C.

Ethyl Ester of 2-Carbethoxy-1-indoleacetic Acid

Phenylhydrazineacetic ester hydrochloride (prepared by Busch's method as above, 30.0 gm.), methyl pyruvate (3) (once distilled, 13.2 gm.), and absolute ethanol (200 cc.) were mixed and saturated with dry hydrogen chloride. The mixture was then heated under reflux for 60 min., cooled slightly, and filtered to remove ammonium chloride; the filtrate was then evaporated under reduced pressure to give a partly-oily, partly-crystalline residue which was thoroughly extracted with ether. The insoluble crystalline residue weighed 4.2 gm. Evaporation of the ethereal extract gave the crude diethyl ester as a dark red syrup in a yield of 92%, based on methyl pyruvate. A small portion of this syrup was fractionally distilled three times to give the following fractions: (1) 1.565 gm., b.p. 120-150°C. at 0.2 to 0.3 mm. (2) 2.308 gm., b.p. 150-155°C. at 0.2 mm. (3) 2.120 gm., b.p. 155°C. at 0.2 mm. Fractions (2) and (3) were pale yellow, viscous oils which slowly crystallized to form long yellow needles. Calc. for $C_{15}H_{17}O_4N$: C, 65.42%; H, 6.23%. Found for fraction (2): C, 65.90, 65.70%; H, 6.25, 6.16%. Greenish-yellow and light red shades were produced by this substance in Ehrlich's test.

2-Carboxy-1-indoleacetic Acid

The crude diethyl ester of this acid (66.7 gm.) was saponified by heating it under reflux for four hours with sodium hydroxide (39.2 gm.) and water (490 cc.). The cooled mixture was extracted with ether; the aqueous layer

was filtered from a small precipitate and then cautiously acidified with concentrated hydrochloric acid, ice being added to keep the temperature down. A light brown precipitate was formed, and was recovered, washed with water, and dried in the air; yield 37.6 gm. or 71%. When the product was taken up in hot alcohol, boiled with charcoal for some time and filtered, and the filtrate treated with several volumes of hot benzene and cooled, sand-colored crystals were recovered in a yield of 25 gm., and further amounts were recovered from the mother liquor. A small portion of this product was further recrystallized twice from water with charcoal and once from benzene–ethanol with charcoal to give the analytical sample of small, white, but not well-shaped, crystals, m.p. 232.8-234.4°C. with decomposition. Calc. for $C_{11}H_9O_4N$: C, 60.27%; H, 4.14%. Found: C, 60.72, 60.33%; H, 4.20, 4.42%. When *asymm*-phenylhydrazineacetic ester hydrochloride made by Harries' method was similarly condensed with almost the theoretical amount of ethyl pyruvate (kindly given to us by Dr. Kulka, Ref. 11), the same diacid was formed on saponifying the intermediate ester, since after purification the acid melted at 234.9-236.0°C., with decomposition, and the analyses were approximately correct. The yield of the crude acid, based on ethyl pyruvate, was 84%. 2-Carboxy-1-indoleacetic acid from either source gave an almost completely negative test with Ehrlich's reagent.

Anhydride of 2-Carboxy-1-indoleacetic Acid

Once-recrystallized 2-carboxy-1-indoleacetic acid (2.02 gm.) and copper chromium oxide catalyst (1) (0.042 gm.) were heated together in a sublimation tube at 0.05 to 0.17 mm. pressure and 178-245°C. The sublimate was powdered and thoroughly extracted with cold aqueous sodium bicarbonate and the insoluble residue (0.32 gm.) was collected, washed, and dried. In a similar experiment, the insoluble sublimate weighed 0.38 gm. The two preparations were recrystallized together from a mixture of isopropyl ether and acetic anhydride. In a third experiment, the same amounts of reactants were used, but the conditions were more drastic. The pressure was held at 200 mm. until the external temperature reached 215°C.; the pressure was then adjusted to 12 mm. and the bath temperature kept at 230-235°C. for 15 min. and up to 245°C. for 10 min. Gas was evolved during this period. The bicarbonate-insoluble sublimate weighed only 0.29 gm. A small portion of it was found to be insoluble in cold caustic solution but soluble in warm caustic solution, from which crystals could then be precipitated by acidification. The rest of the insoluble sublimate from the third experiment was recrystallized from acetic anhydride but much darkening of the material occurred. All of the bicarbonate-insoluble crystals from the three experiments were now united and very cautiously sublimed at a pressure of 0.0005 to 0.005 mm. The sublimate was very thoroughly extracted with aqueous bicarbonate, washed, carefully dried, and recrystallized from a mixture of isopropyl ether (60 cc.) and acetic anhydride (19 cc.), care being taken not to prolong the heating period. The well-formed, light yellow needles were recovered, washed with isopropyl ether, and rigorously dried. Calc. for $C_{11}H_7O_3N$: C, 65.67%;

H, 3.48%. Found: C, 66.26, 66.11, 66.07, 66.15%; H, 3.67, 3.62, 3.85, 3.71%. The crystals had a melting point of 230.5-231.0°C. (uncorr.) with decomposition; their corrected melting point is estimated to be about 237-238°C. from their melting point relative to that of the diacid on the same thermometer. Unchanged diacid was recovered in yields of 48% and 52% in the first two experiments, respectively, but only in low yield in the third.

Acid Amide of 2-Carboxy-1-indoleacetic Acid

Once-crystallized 2-carboxy-1-indoleacetic acid (2.22 gm.) was treated with concentrated ammonium hydroxide (5 cc.) and water (8 cc.) and the mixture was rapidly evaporated to dryness. When the thoroughly dried residue was sublimed at 95-230°C., the pressure of sublimation rose from 0.004 to 0.3 mm. and then fell again to 0.003 mm., showing that gas was evolved. The crystalline residue and sublimate were then treated exactly as before, being even more rigorously dried before sublimation. The sublimate was dissolved in ammonium hydroxide and filtered from a scanty precipitate which was discarded. Acidification of the filtrate gave a solid which was extracted for 30 min. with boiling ethanol (25 cc.); the insoluble material was kept. Evaporation of the alcoholic extract gave a solid which was again treated with ammonium hydroxide, sublimed at a pressure above 0.2 mm., and worked up as before. The alcohol-insoluble material was kept, and the alcohol-soluble material again treated as before, the sublimation being performed at a higher pressure (above 0.2 mm.) and performed more slowly. The combined lots of material insoluble in ethanol but soluble in ammonium hydroxide were recrystallized from ethanol (140 cc.), recovered, dissolved in dilute ammonia, treated with charcoal in the cold, recovered by acidification, and once again treated with ammonia and charcoal as before. The glistening white crystals after thorough washing and drying melted at 272.0-273.6°C. with decomposition. Calc. for $C_{11}H_{10}O_3N_2$: C, 60.55%; H, 4.59%. Found: C, 60.75, 61.20, 60.39%; H, 4.53, 4.40, 4.57%.

Acid Ethyl Ester of 2-Carboxy-1-indoleacetic Acid

Once-recrystallized 2-carboxy-1-indoleacetic acid (33.3 gm.) and absolute ethanol (81 cc.) were warmed to 65°C. and treated with a vigorous stream of hydrogen chloride gas. The crystal cake which formed in about two minutes was broken up; the mixture was warmed to 80°C. and was saturated with hydrogen chloride. Water was added and the mixture was cooled and filtered. The turbid, greasy filtrate was discarded; after being washed and dried the recovered solid weighed 32.0 gm., a yield of 85%. After four recrystallizations from ethanol with charcoal, the material was pure, m.p. 200.5-201.5°C. Calc. for $C_{13}H_{13}O_4N$: C, 63.15%; H, 5.30%. Found: C, 63.37, 62.94%; H, 5.34, 5.57%. The test with Ehrlich's reagent was practically negative.

Anilide of 1-Indoleacetic Acid

Twice-recrystallized acid ethyl ester of 2-carboxy-1-indoleacetic acid, which had been formed from phenylhydrazineacetic ester made by Busch's method, was used. The acid ester (7.0 gm.), quinoline (a redistilled sample of Naugatuck's synthetic material, containing a little aniline, 97 cc.), and copper

chromium oxide catalyst (1) (0.18 gm.) were heated together on an oil bath in an atmosphere of nitrogen. The bath was held at 190°C. for 80 min., at 195-197°C. for 10 min., and at 205°C. for 20 min., then heated briefly to 209°C. The catalyst was removed by filtration; the filtrate was cautiously acidified with dilute hydrochloric acid, ice being added to keep the temperature low. Ether (150 cc.) was added during the acidification. The mixture was filtered and repeatedly extracted with ether; the combined ethereal extracts were washed with dilute hydrochloric acid, with sodium carbonate solution, and finally with water. Evaporation of the ethereal extracts left a brown, gummy residue which was distilled in a Von Braun retort heated in an air bath. Two fractions were obtained: (*a*) an oil which distilled at a bath temperature of 100-130°C. and a pressure of 0.07 to 0.08 mm., yield 2.0 gm., (*b*) crystals which distilled at a bath temperature above 130°C., yield 2.2 gm., m.p. 177.3-178.4°C. A portion (0.48 gm.) of the crystalline fraction was twice recrystallized from dilute ethanol to give the pure anilide of 1-indoleacetic acid as white needles, m.p. 180.3-181.0°C. Calc. for $C_{16}H_{14}ON_2$: C, 76.80%; H, 5.60%. Found: C, 76.81, 76.83%; H, 5.78, 5.80%. Ehrlich's test was positive, several shades of red being produced.

Attempts to decarboxylate the acid ester by heat alone failed, and experiments in which the catalyst was omitted led to very unsatisfactory results.

1-Indoleacetic Acid

(1) The oily fraction of the distillate described just above was heated under reflux for three hours with potassium hydroxide (1.30 gm.), water (2.5 cc.), and ethanol (11 cc.). The solution was concentrated and then made distinctly acid in the cold. White crystals which rapidly began to turn brown were recovered in a yield of 1.58 gm. or 92%. Some ordinary methods of purification failed, but the following procedure was satisfactory. The crude crystals (1.58 gm.) were taken up in ether (75 cc.); the solution was filtered, and the filtrate was allowed to stand in contact with charcoal for two days at room temperature before being filtered again. The filtrate was then evaporated to small volume and treated with five volumes of petroleum ether to give white, fluffy crystals, which turned pink on standing, in a yield of 1.05 gm., m.p. 174.7-175.7°C. Three more similar treatments with charcoal in ether, lasting one day each time, followed by recovery in the same way as before, gave white but not very well formed needles of m.p. 176.3-177.3°C. A final recrystallization from benzene gave the analytical sample, m.p. 178.4-179.4°C., as small, shining needles. Calc. for $C_{10}H_9O_2N$: C, 68.56%; H, 5.18%. Found: C, 68.17, 68.22%; H, 5.34%, 4.96%. Ehrlich's test was strongly positive: a few milligrams of the compound were dissolved in alcohol and treated with an alcoholic solution of *p*-dimethylaminobenzaldehyde to give a yellow solution. Addition of a few drops of concentrated hydrochloric acid gave a medium red color which changed to a ruby red when the mixture was heated. Cooling did not alter the color but the addition of sodium nitrite gave a very dark red solution not changed by heating or cooling.

(2) The crude anilide of 1-indoleacetic acid (obtained in the second fraction

of the distillate described in the previous section, 1.32 gm.) was heated under reflux for three hours with potassium hydroxide (0.70 gm.), water (1.2 cc.), and ethanol (6.0 cc.). Two products were eventually isolated in the usual way: a basic oil which was identified as aniline by converting it to benzenesulphonanilide, m.p. 109-110°C. (uncorr.), and acidic crystals, m.p. 174.7-176.3°C., mixed m.p. with 1-indoleacetic acid 174.7-176.8°C., which were therefore not quite pure 1-indoleacetic acid. This experiment confirmed the constitution of the anilide of 1-indoleacetic acid.

Pyrolysis of 2-Carboxy-1-indoleacetic Acid

Pyrolysis of the diacid at very low pressures in the presence of a catalyst led only to the partial conversion of the acid to its anhydride, as already described. Pyrolysis of the diacid alone at ordinary pressure produced a tar which yielded no pure products, as well as very small amounts of an oily distillate thought to be N-methylindole and of a crystalline sublimate thought to be crude 1-indoleacetic acid. When 2-carboxy-1-indoleacetic acid (1.50 gm.) was heated with quinoline (7.2 cc.) and copper chromium oxide catalyst (0.043 gm.), some impure 1-indoleacetic acid was obtained, but considerable amounts of tar were formed as well. Better results were obtained when the diacid (3.48 gm.) was heated with quinoline (54 cc.) and copper chromium oxide catalyst (0.101 gm.), since very little tar was formed and 1-indoleacetic acid was recovered by the method already described; after three years it had a melting point of 176.3-177.8°C. This acid was not analyzed, but the pyrolyses of the diacid in quinoline also yielded neutral crystals of m.p. 181.0-182.0°C. and mixed m.p. with the anilide of 1-indoleacetic acid already described, 180.0-181.5°C. Calc. for $C_{16}H_{14}ON_2$: C, 76.80%; H, 5.60; N, 11.20%. Found: C, 76.22, 75.94, 77.17%; H, 5.57, 5.61, 5.64%; N, 11.03, 10.98%. Since the anilide made in the experiments of this section had been formed from phenylhydrazineacetic ester made by Harries' method, the mixed melting point with the anilide described previously was confirmation also of the identity of the phenylhydrazineacetic esters made by the method of Harries (6) and of Busch (2).

2-Carboxy-3-methyl-1-indoleacetic Acid, Diethyl Ester

α-Ketobutyric acid was formed in excellent yield from crotonic acid by the method of Pfister, Robinson, and Tishler (13), and then converted to its methyl ester in 51% yield by the elegant general method of Clinton and Laskowski (3). Crude phenylhydrazineacetic ester hydrochloride (made by Busch's method, 36.0 gm.), methyl α-ketobutyrate (b.p. 66-69.5°C. at 26 mm., 18.0 gm.), and absolute ethanol (240 cc.) were then mixed, saturated with dry hydrogen chloride, heated under reflux for one hour, cooled slightly, and filtered; the precipitated ammonium chloride weighed 6.0 gm. The filtrate deposited a heavy crop of crystals on standing, and a further crop was obtained by evaporating the mother liquors. Extraction of the combined crystal crops with ether gave the crude diethyl ester as very light brown crystals (soluble in ether) in a yield of 38.3 gm. or 86% based on methyl α-ketobutyrate. When a small sample was thrice recrystallized from ethanol, charcoal being

used twice, white, well-formed needles of m.p. 80.0°C. (uncorr.) were obtained. Calc. for $C_{16}H_{19}O_4N$: C, 66.42%; H, 6.62%. Found: C, 66.88, 66.54%; H, 6.40, 6.57%. The material gave a practically negative test with Ehrlich's reagent.

2-Carboxy-3-methyl-1-indoleacetic Acid

The crude diethyl ester (36.3 gm.) was saponified in the usual way with aqueous alcoholic sodium hydroxide, and the crude dicarboxylic acid was obtained in 93% yield. When a small portion was recrystallized twice from benzene–ethanol and twice from dilute ethanol with charcoal, pure 2-carboxy-3-methyl-1-indoleacetic acid was obtained in well-formed, shining crystals of m.p. 236.5-237.6°C. with decomposition. Calc. for $C_{12}H_{11}O_4N$: C, 61.80%; H, 4.75%. Found: C, 61.67, 61.43%; H, 4.81, 4.90%. The test with Ehrlich's reagent was practically negative.

Acid Ethyl Ester of 2-Carboxy-3-methyl-1-indoleacetic Acid

The crude acid obtained as above (22.1 gm.) was mixed with absolute ethanol (50 cc.), warmed to 65°C., and treated with dry hydrogen chloride. The crystal cake was then broken up, treated with an additional 10 cc. of absolute ethanol, warmed to 80°C., and saturated with hydrogen chloride. Deep blue crystals having an extremely foul odor were recovered from the red, turbid, diluted alcoholic medium, and dried to give 21.8 gm. (88%) of the crude half ester. Three recrystallizations of the product from ethanol with charcoal gave colorless but not well-formed crystals which had a sweet odor. One more recrystallization of a small portion of these crystals from a large amount of ethanol gave the analytical sample of m.p. 195.7-196.7°C. Calc. for $C_{14}H_{15}O_4N$: C, 64.34%; H, 5.79%. Found: C, 64.88, 64.62, 64.81%; H, 5.79, 5.88, 5.64%. The test with Ehrlich's reagent was negative.

Decarboxylation of the Acid Ethyl Ester of 2-Carboxy-3-methyl-1-indoleacetic Acid

The half ester described above (thrice crystallized, 7.0 gm.), quinoline (Naugatuck's redistilled, 31.0 cc.), and copper chromium oxide catalyst (0.17 gm.) were heated together at a bath temperature of 180-190°C. for 80 min., at 190-200°C. for 10 min., and at 200-204°C. for 15 min. The mixture was then filtered, cooled, treated with ether, and acidified in the cold with dilute hydrochloric acid, again filtered, and then thoroughly extracted with ether. Very little tar was produced in the reaction. After the combined ethereal extracts had been washed with dilute hydrochloric acid, with sodium carbonate solution, and with water, they were evaporated to leave a semisolid, brown residue which was distilled at 0.06 mm. pressure in a von Braun retort. The following fractions were obtained: (1) distilled at a bath temperature of 95-110°C., an oil; (2) bath temperature 110-116°C., yield 1.585 gm., an oil; (3) bath temperature 116-165°C., an oil; the total yield of the first three fractions was 4.376 gm.; (4) bath temperature 165-250°C., yield 0.486 gm., a solid; (5) tarry residue, 0.19 gm.

The crystalline fraction (4) (0.486 gm.), together with 0.129 gm. of distilled crystals from a similar run, was recrystallized from hot ethanol (30 cc.) to

give 0.346 gm. of crystals of m.p. 219.7-223°C. Evaporation of the mother liquor yielded a brown gum, so that this fraction of the distillate was not homogeneous. Two more recrystallizations of the crystals from ethanol gave very white crystals of m.p. 221.9°-222.4°C. whose analysis showed them to be the anilide of 3-methyl-1-indoleacetic acid. Calc. for $C_{17}H_{16}ON_2$: C, 77.25%; H, 6.10%. Found: C, 77.34%; H, 6.33%. Light amber and pink shades were produced with this material in Ehrlich's test.

The oily fraction (2) of the distillate (1.585 gm.) was redistilled, and the oily central fraction distilling at a bath temperature of 112-115°C. at 0.06 mm. was collected and analyzed. Calc. for $C_{13}H_{15}O_2N$: C, 71.86%; H, 6.96%. Found: C, 72.03, 72.34%; H, 7.19, 7.13%, showing it to be ethyl 3-methyl-1-indoleacetate. Ehrlich's test on the material produced successively deep pink, light red, brown, and purple shades.

3-Methyl-1-indoleacetic Acid

(1) The crude ethyl ester of this acid (3.72 gm. from the first three fractions of the distillate described in the previous section, together with 1.50 gm. from a similar experiment) was saponified in aqueous alcoholic potassium hydroxide and the product was recovered in the usual way. The crude acid was obtained in a yield of 2.624 gm. or 58%, m.p. 175.2-177.8°C. with slight decomposition. It had a foul odor and turned light brown when dried but was noticeably more stable than 1-indoleacetic acid. The crude acid was dissolved in ether, treated for several hours with two successive portions of charcoal, separated from the charcoal, and precipitated with petroleum ether. Two further recrystallizations of the product from benzene gave very white crystals of m.p. 178.9-179.9°C. Calc. for $C_{11}H_{11}O_2N$: C, 69.82%; H, 5.86%. Found: C, 69.68, 69.90%; H, 6.02, 5.83%. Red, amber, and violet shades were obtained with this material in Ehrlich's test.

(2) Crude 1,3-indoleacetic acid (m.p. 232°C., 0.658 gm.), kindly given to us by Dr. R. H. Manske, was melted at atmospheric pressure and immediately distilled at 0.5 mm. pressure. The distillate was purified in the usual way, but unfortunately its melting point could not be raised above 174-176°C. In microscopic appearance and in odor it was identical with the 3-methyl-1-indoleacetic acid made by method (1) and on admixture with the latter (which after several months also melted a few degrees below its true melting point) it caused no depression of the melting point. Jackson and Manske (8) obtained a melting point of 178°C. for the acid made in this way.

Biological Tests (17)

Young tomato plants were purchased on the Kingston market and grown under vertical light until they were 8 to 12 in. high. Each plant was then photographed, treated on the upper sides of the leaf petiole and on one side of the adjacent stem with a solution of an analytically pure indole derivative (15 mgm.) in lanolin (1 gm.), and kept in darkness at night and under vertical light by day. The plants were photographed at intervals and the change in the angle between petiole and stalk was measured on the photographs. Under these conditions, the well-known growth regulator 3-indoleacetic acid pro-

duced marked induced cell elongation in 24 hr., with little further change occurring after five days. The anilide of 1-indoleacetic acid had an effect about two-thirds as great, but produced it equally quickly. Smaller and more slowly induced elongations were given by the half esters of 2-carboxy-1-indoleacetic acid and of 2-carboxy-3-methyl-1-indoleacetic acid, and by the diethyl ester of 2-carboxy-3-methyl-1-indoleacetic acid, while the elongation produced by the diethyl ester of 2-carboxy-1-indoleacetic acid was slight. The plants treated with 1-indoleacetic acid, 3-methyl-1-indoleacetic acid, 2-carboxy-1-indoleacetic acid, and 2-carboxy-3-methyl-1-indoleacetic acid all withered and turned brown after about one day; during this time slight cell elongation occurred with the first and fourth of these acids but not with the other two.

ACKNOWLEDGMENTS

The authors wish to thank Dr. R. H. Manske for suggesting this problem to them and for his highly valued advice during the early stages of their work. The encouragement which they received from Dr. J. A. McRae in the later development of the problem was much appreciated. Dr. Manske, Dr. Kulka, and Dr. Gillies of the Dominion Rubber Company are thanked for gifts of chemicals, and Mr. Ralph Mills of the same Company is thanked for performing a few of the analyses here recorded.

REFERENCES

1. ADKINS, H. Reactions of hydrogen. University of Wisconsin Press, Madison. 1946. p. 12.
2. BUSCH, M. Ber. 36: 3877. 1903.
3. CLINTON, R. O. and LASKOWSKI, S. C. J. Am. Chem. Soc. 70: 3135. 1948.
4. FINDLAY, S. P. and DOUGHERTY, G. J. Org. Chem. 13: 560. 1948.
5. FISCHER, E. and HESS, O. Ber. 17: 559. 1884.
6. HARRIES, C. D. Ber. 28: 1223. 1895.
7. HARTMAN, W. W. and ROLL, L. J. *In* Organic syntheses: Collective Vol. 2. John Wiley and Sons, Inc., New York. 1943. p. 418.
8. JACKSON, R. W. and MANSKE, R. H. Can. J. Research, B, 13: 170. 1935.
9. KERMACK, W. O., PERKIN, W. H., JR., and ROBINSON, R. J. Chem. Soc. 119: 1602. 1921.
10. KING, F. E. and L'ECUYER, P. J. Chem. Soc. 1901. 1934.
11. KULKA, M. Can. J. Research, B, 24: 221. 1946.
12. MOUILPIED, A. T. de. J. Chem. Soc. 87: 435. 1905.
13. PFISTER, K., ROBINSON, C. A., and TISHLER, M. J. Am. Chem. Soc. 67: 2269. 1945.
14. REISSERT, A. Ber. 28: 1230. 1895.
15. SCHROETER, G. Ann. 418: 161. 1919.
16. TANAKA, Z. J. Pharm. Soc. Japan, 60: 74. 1940. Chem. Abstracts, 34: 3735. 1940.
17. ZIMMERMAN, P. W. *In* Growth of plants. *Edited by* Crocker, W. Reinhold Publishing Corporation, New York. 1948. p. 204.

ON THE LIQUID–VAPOR COEXISTENCE CURVE OF XENON IN THE REGION OF THE CRITICAL TEMPERATURE[1]

By M. A. Weinberger[2] and W. G. Schneider

ABSTRACT

The liquid–vapor coexistence curves of very pure xenon have been determined in bombs of vertical lengths 1.2 cm. and 19 cm. The longer bomb yielded a flat-topped coexistence curve, the shorter a more rounded curve. The classical van der Waals theory is capable of explaining a large portion of the flat top if effects of gravity are taken into account. Details of the theoretical variation of the width of the flat top with vertical bomb lengths are given. The critical data obtained for xenon are $\rho_c = 1.105$ gm./cc., $T_c = 16.590 \pm .001$°C. The danger of contamination of gases in the critical region on contact with gasket or packing materials is stressed.

INTRODUCTION

At the present time the true nature of the liquid–vapor coexistence curve in the vicinity of the critical temperature is not known. According to some workers, the top of the coexistence curve is horizontal over a finite density range (16,9,11,14), and differs in this respect from the classical Andrews–van der Waals curve, which is roughly parabolic and gives rise to a unique critical density. A knowledge of the true shape of the coexistence curve (as well as the PV isotherms) is essential for assessing the several theoretical treatments of the critical point, and in particular the condensation theory of Mayer (10). It was concluded on the basis of this theory that the top of the observable coexistence curve is horizontal over a finite density range, and moreover, above the maximum coexistence temperature and extending over a small interval of temperature, the PV isotherms are horizontal. Today, 15 years later, it is still not possible to say with certainty whether these derived properties correspond to any real system.

Recently an investigation of the coexistence curve (2) and the isotherms (8) of sulphur hexafluoride was carried out. The top of the coexistence curve appeared more rounded than flat and the isotherms immediately above the critical temperature had a small but finite slope. Unfortunately the coexistence curve measurements did not cover a sufficiently wide density range to include also the "wings" of the curve (where the meniscus vanishes at the top or bottom of the containing bomb), and the large scale used in plotting the coexistence temperatures over the small density range studied tended perhaps to exaggerate the "roundness" of the curve. After these results were reported, it became apparent from further measurements that the effects of the gravitational field had not been properly taken into account. Accordingly, it seemed desirable to carry the investigations further and in particular to study the influence of gravitational effects.

[1] *Manuscript received February 8, 1952.*
Contribution from the Division of Chemistry, National Research Laboratories, Ottawa, Canada. Issued as N.R.C. No. 2724.

[2] *National Research Council of Canada Postdoctorate Fellow. Present address: Defence Research Chemical Laboratories, Ottawa, Canada.*

The large effect of gravity on a system in the critical region is due to its very large compressibility. Hence, the weight of the medium itself will cause density gradients to be set up. This was pointed out as early as 1892 by Gouy (4) and calculations of the effect have also been given by Ruedy (15). In spite of this, no attempt appears to have been made to account for the observed coexistence curves from this point of view. Because of the S-shaped nature of the critical isotherm, the largest density gradient will occur at that height in the tube where the meniscus disappeared. This has been amply demonstrated by the work of Maass and co-workers (7). Moreover, if there exists for each gas a unique critical density and a unique critical temperature which correspond, as in the classical theory, to the maximum of the coexistence curve and to the point of inflection of the critical isotherm, then it follows that: (1) For a long vertical bomb, as the over-all filling density is varied, the unique critical density will be realized at varying heights within the bomb, and at each height the meniscus will disappear at the same temperature giving rise to a flat-topped coexistence curve. The critical isotherm (obtained by measuring pressures at the position of the meniscus) must therefore also be horizontal over the same range of densities.

(2) For an infinitely short tube, the effect of gravity should be negligible, and the critical phenomena should be observable at a single density only. At this density there would be a point of inflection on the isotherm and at all other densities the slope of the isotherm would be finite.

(3) The coexistence curve obtained with a long vertical bomb should lie entirely outside that obtained with a very short bomb. This is because in the long bomb, the liquid phase, owing to the action of gravity, is more compressed, i.e., has a greater mean density, and the vapor phase has a smaller mean density than in the case of a very short bomb. At temperatures below the critical, where the effect of gravity is proportionately less, the two coexistence curves would merge.

In the present experiments the effect of gravity on the shape of the coexistence curve was demonstrated by using a long bomb and a very short one, obtained by turning a bomb of the usual type on its side. The measurements were carried out with very pure xenon. Gravitational effects with this gas would be expected to be large because of its high density. Furthermore, the coexistence curve data for a monatomic gas were needed in connection with other measurements in the critical region now in progress.

EXPERIMENTAL

Purity of Xenon

Two different samples of xenon were procured. The first sample, which was used for the earlier experiments, was obtained from the Linde Air Products Company. After several fractional distillations, mass spectrometer analyses showed a krypton content of between 0.1 to 0.3% and no other impurities.

The second sample of xenon was obtained from the General Electric Company. This sample was stated to contain less than a hundred parts per million

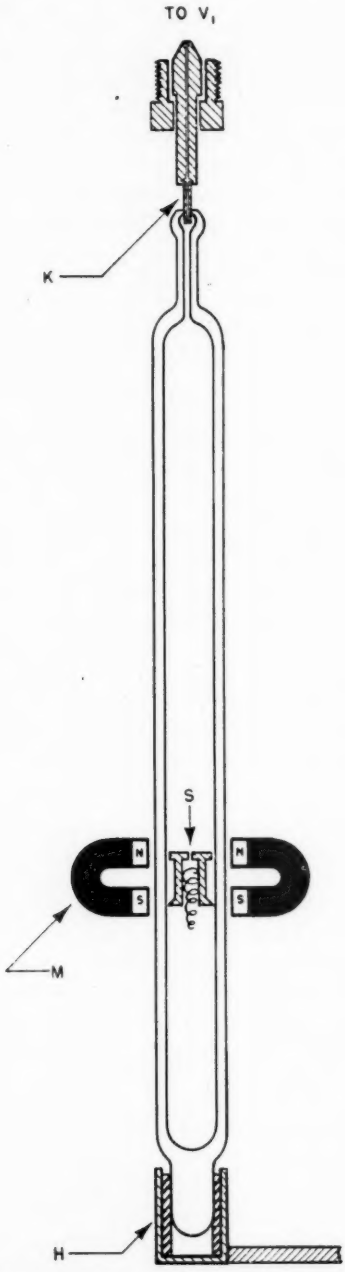

FIG. 1. Diagram of observation bomb.

of krypton. No detectable amounts of krypton (i.e., less than 0.01%) or any other impurities could be found on analysis with a mass spectrometer.* All the experimental results quoted here were obtained with this sample of xenon.

Design of Bomb

The original design of the glass bomb was similar to that used by Atack and Schneider (1,2). The bomb contained a helical glass stirrer and was attached to a high pressure valve by means of a gland nut seating on neoprene. With this arrangement the neoprene gaskets were exposed to the gas at high pressure inside the bomb. It was found that on emptying the bomb at the end of an experiment, oily droplets were invariably deposited on the bottom end of the bomb. The conclusion was reached that xenon at high pressure dissolved materials from the neoprene.

Use of a Kovar-glass seal *K* to join the glass bomb to the metal part fitting into the shut-off valve (Fig. 1) overcame this difficulty. This type of bomb was used in all the experiments quoted. Provided the Kovar and graded seals to the pyrex bomb were well annealed and the clamping in the thermostat introduced no strain, the bombs stood up well to pressures of approximately 1000 lb. per sq. in.

For experiments with the bomb in a vertical position a slug *S* made of Swedish iron was used for magnetic stirring (Fig. 1). The hollow slug having an orifice in its top end forced up a jet of fluid on falling.† Care was taken to minimize oxidation of the slug whilst making the bomb. For the bomb in a horizontal position a helical glass stirrer with a glass encased nail in the center was used. In both cases stirring was achieved by two small permanent magnets on either side of the bomb which were appropriately moved. This had the advantage over solenoid stirring in that the whole length of the bomb could be seen and the danger of local heating by the solenoid was eliminated.

The volumes of the bombs were measured to one part in a thousand by a gas expansion method described by Kaminsky and Blaisdell (6). The dimensions of the bombs were as follows:

Vertical bomb:	Length (exclusive of connecting capillary) 19.5 cm.
	I.D. 9 mm.
	Volume 11.49 cc.
Horizontal bomb:	I.D. 12 mm. (vertical height)
	Volume 10.70 cc.
	Horizontal length 14 cm.

Method

The procedure followed in obtaining the coexistence curve data was similar to that used previously (2). The glass observation bomb was initially filled to some predetermined density greater than the critical; the density was then varied in small decrements by bleeding off a measured amount of gas. At each density observations of the temperature of meniscus disappearance on

* *We have very recently been informed that the Linde Air Products Company is now able to supply xenon of a comparable purity.*

† *This design was suggested to us by Mr. S. G. Whiteway of McGill University, Montreal, Que.*

heating and reappearance on cooling were made. At the higher densities at which the meniscus did not disappear within the tube, the temperature at which the last bubble of vapor was seen to disappear at the top of the tube was taken; at the low densities, the temperature at which the last drop of liquid disappeared at the bottom of the tube was measured. In this manner the "wings" of the coexistence curve were obtained.

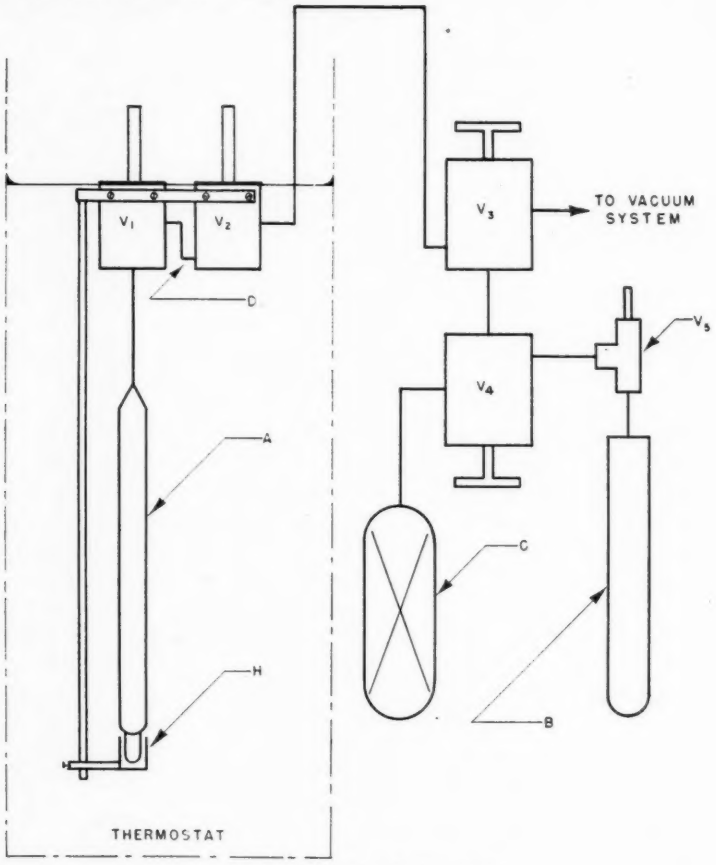

FIG. 2. Diagram of apparatus.

A diagram of the apparatus is shown in Fig. 2. The valves V_1, V_2, V_3, and V_4 were high pressure steel needle valves with Teflon packing. The brass weighing bomb B was fitted with a specially designed light-weight shut-off valve, V_5.

The method of filling the observation bomb, A, with xenon, adopted at first, led to some difficulty and is worth mentioning here because it has undoubtedly introduced some error into other experimental data on critical properties. A weighed amount of xenon (in excess of that required to fill the

glass bomb) was introduced into the weighing bomb, *B*. With the temperature of the glass bomb held 5° below the critical temperature, the gas from the weighing bomb at 90°C. was permitted to distill into the glass bomb until the latter was approximately two-thirds filled with liquid. The gas remaining in the capillary lines was then condensed back into the weighing bomb with liquid nitrogen. Reweighing the weighing bomb gave the amount of gas transferred to the glass bomb. The density decrements were obtained by expanding the gas from the glass bomb into the capillary tube, *D*, and then condensing it into the weighing bomb. The change in density was obtained from the increase of weight in the weighing bomb and the known volume of the glass bomb.

In a series of measurements with separate fillings of the glass bomb by the above procedure, it was found that the coexistence temperatures observed for replicate fillings differed by as much as 0.1°C. Moreover on condensing out the remaining gas at the end of the experiments, small "oily" droplets were observed on the inner surface of the glass bomb. (This deposit was in appearance similar to that observed previously when a small neoprene gasket was used in the earlier type of bomb.) It was concluded that the contamination resulted from the above method of filling the tube. During the filling the gas is at a temperature and pressure approaching the critical values, and is in contact with the Teflon packings of the needle valves in the system for a relatively short period of time (10-20 min.). A gas near the critical region is known to be a good solvent and it is believed that in the present case the oily material (possibly a plasticizer or depolymerization product) was dissolved out of the Teflon packing. Accordingly all subsequent fillings were carried out by condensing the gas from the weighing bomb into the glass bomb at low pressures (less than 10 mm.) controlled by surrounding both vessels with liquid nitrogen. The subsequent method of changing the densities was the same as described above. With this procedure no deposit could be detected in the glass bomb at the end of the experiment, and successive experiments yielded coexistence temperatures when the liquid meniscus disappeared within the tube, agreeing to within one or two thousandths of a degree.

This experience serves to emphasize the necessity of eliminating all packing or gasket material which may contain contaminants, e.g., rubber, Teflon, leather, from direct contact with the high pressure gas even for short periods of time. In the present work the shut-off valves on the glass bomb and the weighing bomb, V_1 and V_5, were so connected that the gas within the bombs was in contact with the steel stem of the valve, and not with the packing.

Before condensing the gas into the glass bomb it was thoroughly evacuated and flushed with small amounts of xenon. The brass holder, *H* (Fig. 1), at the bottom of the bomb was then disconnected and the slug *S* raised to the top of the tube with the magnets. The bomb could then be surrounded with liquid nitrogen to condense the gas. When the filling was completed, the liquid nitrogen was removed and the holder *H* was attached while the bomb was still cold. As it warmed up moisture condensed on the outside surface and

when this began to melt the thermostat was immediately filled with ice water. This procedure minimized the possibility of thermal shocks to the glass tube. The thermostat was then heated to the desired temperature.

The weighing bomb *B* had a volume of 23 cc. and a tare weight of 275 gm. After the bomb was repeatedly cooled in liquid nitrogen, warmed up, dried and wiped, the weight could be reproduced to 0.5 mgm. The average weight of xenon added to the weighing bomb on a single expansion from the glass bomb was approx. 0.28 gm. It is estimated that, taking into account the error in the volume calibration of the glass bomb, the error in the density determinations does not exceed 0.2%. A small cumulative error was introduced owing to the fact that a small pressure of gas equal to the vapor pressure of xenon at $-$ 195°C. (3×10^{-2} mm. Hg) (13) remained in the connecting line when the gas was condensed into the weighing bomb with liquid nitrogen. This error was minimized by reducing the volume of the connecting capillary to a small value. The pressure in this volume was monitored with the thermocouple gauge *C* (Fig. 2). The difference in the total weight of gas introduced into the glass bomb and the total weight recovered at the end of the experiment did not, on the average, exceed 10 mgm. for a charge of $\sim$ 15 gm. xenon.

Temperature Control

The water-filled thermostat of capacity 15 gal. was very rapidly stirred by propeller and centrifugal pump stirrers. The required temperature was reached by equilibrating the cooling provided by coils wound around the outside of the bath (through which cooled glycol–water mixture circulated) with the heat liberated by a 60 watt knife-edge immersion heater. An auxiliary 250 watt heater was used for rapid heating.

The regulator consisted of two glass encased thermistors (No. 14B Western Electric) connected in parallel in the arms of a Wheatstone bridge. The out-of-balance of the bridge was indicated by a sensitive mirror galvanometer using a 4 meter light path. The light from the galvanometer actuated a photocell-relay circuit which controlled the heating current. This straight on–off heating was found to be quite satisfactory and temperature constancy of $\pm$ 0.001°C. for periods of hours and $\pm$ 0.0005°C. for shorter periods was achieved.

The actual bath temperature was measured with a platinum resistance thermometer. To check the thermometer calibration, ice points were taken after each reading.

RESULTS

Observation of Coexistence Temperature

The bomb was observed by transmitted light from an ordinary fluorescent lamp. The methods of observation differed according to whether the meniscus disappeared within the tube or went out through the top or bottom of the bomb, or whether the bomb was vertical or horizontal.

Vertical Bomb

(*a*) High Density Range

With continuous stirring of the bomb contents, the bath was heated very slowly till the meniscus and any white mist above it had reached the very top of the bomb capillary. The temperature was raised a little more and the bath then allowed to cool slowly while the system was still stirred. The temperature was taken at which there was simultaneous cloudiness and meniscus formation at the very top of the capillary.

As the liquid may not have completely filled the metal capillary leading to the valve, the coexistence temperatures corresponding to high densities suffer from a larger error than those for medium and low densities. As, however, the curve is very steep in this region this error should not materially affect the general shape of the curve.

No yellow or brownish opalescence was observed in this region.

(*b*) Medium Density Range

Here the meniscus disappeared within the bomb. In this region a yellow-brown opalescence was always present.

The general behavior of the system in this region was as follows. Starting at a temperature at which a sharp line separating liquid and vapor phases was definitely visible, this line gradually became broader on heating without stirring. The fluid then consisted of pale yellow top and bottom regions and a brown middle region. On cooling without stirring, condensation set in from the top of the bomb and the yellow fog produced settled towards the meniscus region. When getting near (~ 0.003°C.) the coexistence temperature the condensation from the top of the bomb became suddenly very heavy and settled out to a narrow deep brown band. This at a somewhat lower temperature settled to become a sharp line separating the liquid and vapor phases.

The method used for measuring the coexistence temperature was to heat the xenon with stirring to about $0.002 - 0.003$°C. above the temperature at which the sharp separation line was present. Stirring was stopped and the system was allowed to stand at this temperature. When a diffuse brown band had settled after periods of one-half to one hour the temperature was lowered in steps of 0.001°C. with stirring. After each step the gas was allowed to stand till ultimately, when the cooling had been sufficient, a sharp separation line was obtained. This temperature was taken. The fluid was then cooled further with stirring and then reheated in steps of 0.001°C. being allowed to stand after each 0.001°C. rise in temperature till the phase separation line became hazy.

The cycle of heating and cooling was repeated till reproducible temperatures of formation and disappearance of the sharp separation line were obtained which in general agreed to 0.001°C. This temperature was taken as the coexistence temperature.

(*c*) Low Density Range

Here the meniscus went out through the bottom of the bomb. In this range, as

in the high density range, no yellow opalescence was observed. On heating it sufficiently the fluid became quite clear. After cooling the fluid with stirring a temperature was reached where, after the system was allowed to stand, a slight wisp of white mist was seen on the very bottom of the tube when stirring was recommenced. A meniscus could sometimes be seen too. The cycles of heating and cooling were repeated till the temperatures of reappearance or disappearance of the mist were bracketed closely. The precision of these coexistence temperatures was also not as high as those for the medium range.

Horizontal Bomb

The bomb which had a plane heavy glass window sealed on one end was mounted horizontally, and observations of the meniscus were made through the end window.

(*a*) High Density Range

In this region there was no opalescence. Observations were taken while stirring. On heating sufficiently with stirring the vapor region was transformed into bubbles like those in a spirit level and these ultimately disappeared. The bath was then cooled, whereupon small bubbles followed by larger ones reappeared. The cooling and heating cycles were repeated till the temperatures of disappearance and reappearance of the bubbles agreed to about 0.005°C. The average was taken as the coexistence temperature.

(*b*) Medium Density Range

Owing to the angle from which the end of the tube was viewed the appearance of opalescence in this region was quite different from that observed with the bomb in the vertical position. At the coexistence temperature the xenon had, by transmitted light, and when viewed along the long axis of the tube, a brass color at the beginning and end of the medium density range which deepened to clear orange and very dark red in the center of the range. The colors were so intense that it was usually impossible to see the sharp separation line which had been taken as the criterion for the coexistence temperature in the case of the vertical bomb. However, it was found that the onset or disappearance of clouding of the clear deep red system on cooling or heating with stirring was very sudden and reproducible, and repetition of the heating and cooling cycle enabled the temperature at which this occurred to be bracketed to within 0.001°C. This clouding temperature was taken as the coexistence temperature.

(*c*) Low Density Range

The system again appeared colorless in this region and the mean temperature of onset and disappearance of cloudiness was taken as the coexistence temperature.

The results of duplicate runs with the bomb in the vertical position and the run with the horizontal bomb are shown in Table I.

The whole coexistence curve is shown in Fig. 3 and a larger scale plot of the medium density range is shown in Fig. 4. The positions of the arrows indicate roughly the extremities of the region of opalescence.

TABLE I

Vertical bomb						Horizontal bomb		
Density, gm./cc.	Coexistence temp., °C.	Remarks	Density, gm./cc.	Coexistence temp., °C.	Remarks	Density, gm./cc.	Coexistence temp., °C.	Remarks
		↑ Meniscus goes out through top of bomb			↑ Meniscus goes out through top of bomb	1.437	14.984	↑
			1.339	15.917		1.370	15.722	
			1.316	16.107		1.322	16.093	Meniscus goes out through top of bomb
			1.291	16.329				
			1.267	16.479		1.274	16.335	
1.250	16.579	↓	1.240	16.563	↓			↓
						1.226	16.494	
			1.190	16.592	↑	1.203	16.544	↑
1.173	16.589	↑				1.177	16.569	
			1.164	16.592				↓
1.148	16.590					1.152	16.583	↑
					Region of opalescence			Region of opalescence
			1.138	16.591				
		Region of opalescence			↓	1.127	16.588	↓
1.122	16.589				Meniscus disappears within bomb			Meniscus disappears in bomb
		Meniscus disappears within bomb	1.113	16.591	↓			↓
						1.101	16.588	
1.097	16.589	↓						
			1.088	16.591		1.077	16.582	
1.072	16.587							
			1.062	16.591		1.052	16.580	
1.046	16.586					1.028	16.560	↑
			1.015	16.588				
						1.004	16.529	
			0.990	16.586	↓			↓ Meniscus goes out through bottom of bomb
		↑				0.980	16.476	
0.966	16.500				↑			
			0.965	16.540				
		Meniscus goes out through bottom of bomb			Meniscus goes out through bottom of bomb	0.933	16.303	
			0.932	16.374				
			0.907	16.255				
						0.878	16.022	
			0.862	15.907				
0.825	15.383	↓			↓	0.845	15.636	↓

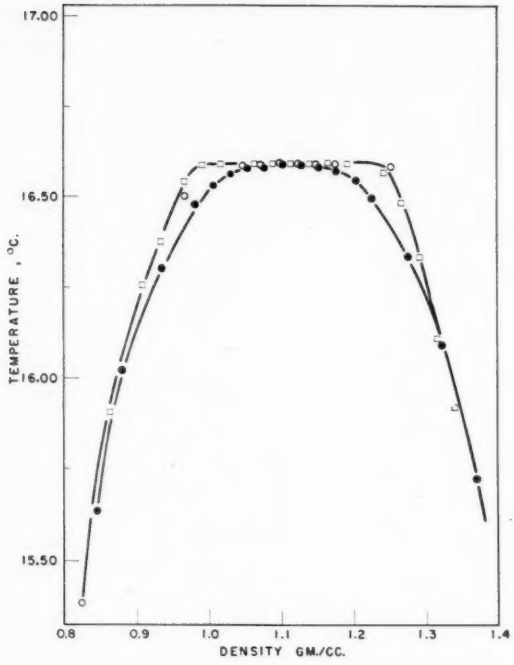

FIG. 3. Coexistence curves of xenon. ○, □ vertical bomb. ● horizontal bomb.

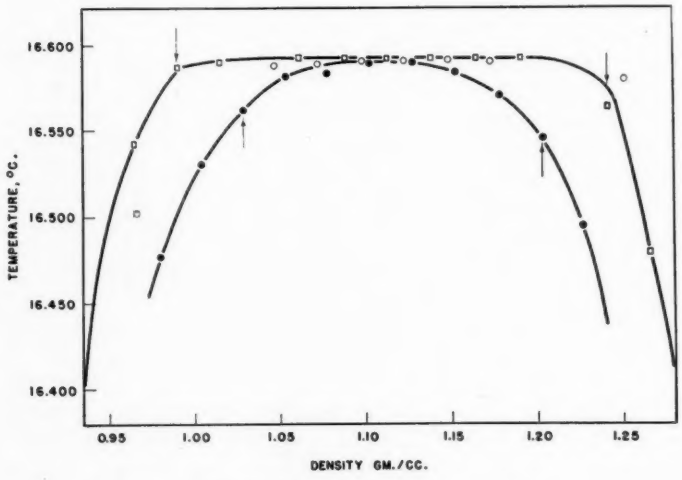

FIG. 4. Larger scale plot of coexistence curves of xenon.

The critical temperature and density were obtained by application of the law of rectilinear diameters. They are:

$$\rho_c = 1.105 \text{ gm./cc.}$$

$$T_c = 16.590 \pm 0.001°\text{C.}$$

The only values in the literature for comparison are those of Patterson, Cripps, and Whytlaw-Gray (12):

$$\rho_c = 1.155 \text{ gm./cc.}$$

$$T_c = 16.6°\text{C.}$$

DISCUSSION

As may be seen from Figs. 3 and 4 there is a striking difference in the appearance of the coexistence curves for bombs in the vertical and horizontal positions. The curve obtained from vertical bomb data has steeply rising wings which are, however, truncated at the flat top corresponding to the constant temperature of meniscus disappearance at the various densities. The curve using the horizontal bomb is more rounded and the truncated region is very much smaller. These results demonstrate the marked influence of gravity on the nature of the coexistence curve. The general characteristics of the observed curves are qualitatively, at least, in good agreement with the classical theory when due account is taken of gravitational effects (see Introduction).

It is of interest to estimate the extent of the flat top in terms of the vertical length of the bomb. It will be assumed that because of the hydrostatic effect there will be a continuous variation of density and pressure with height and that, in the times taken for observation, equilibrium has been reached with respect to this variation.

It is further assumed that there are unique critical parameters, P_c, ρ_c, and T_c, corresponding to the maximum of the rounded top which would be obtained with a bomb of infinitely small length. It then follows that if a bomb of finite length, filled at some density near the critical density, ρ_c, is held at the critical temperature, T_c, there will be only one height at which the critical parameters are exactly realized and at this height the meniscus will be observed to disappear. There will therefore be a range of mean filling densities over which the meniscus will disappear at various heights within the bomb at the critical temperature, T_c. This range of mean densities, $\Delta\bar{\rho}$, which is dependent on the height or length of the bomb, extends from the mean density, $\bar{\rho}_1$ which yields the critical density ρ_c at the top of the bomb to that ($\bar{\rho}_2$) giving ρ_c at the bottom

of the bomb. Anywhere within this range $\bar{\rho}_1$ to $\bar{\rho}_2$ the system will attain the critical density ρ_c at some point within the bomb.

To calculate the extent of the flat top $\bar{\rho}_1 - \bar{\rho}_2$ we note that for a bomb of uniform cross section

$$\bar{\rho}_1 = \frac{1}{L}\int_0^L \rho_h dh \quad \text{with } \rho_L = \rho_c$$

where L is the (vertical) length of the bomb, ρ_h the density at height h, and zero height taken at the bottom of the bomb.

Replacing the integral by a sum we have

$$\bar{\rho}_1 \doteq \frac{1}{L}\sum_{\rho_o}^{\rho_T=\rho_c} \rho_h \delta h$$

and similarly,

$$\bar{\rho}_2 = \frac{1}{L}\int_0^L \rho_h dh \doteq \frac{1}{L}\sum_{\rho_o=\rho_c}^{\rho_L} \rho_h \delta h \quad \text{with } \rho_o = \rho_c.$$

Hence,

$$\Delta\bar{\rho} = \bar{\rho}_1 - \bar{\rho}_2 \doteq \frac{1}{L}\left\{\sum_{\rho_o}^{\rho_L=\rho_c} \rho_h \delta h - \sum_{\rho_o=\rho_c}^{\rho_L} \rho_h \delta h\right\}.$$

To obtain values for ρ_h the critical isotherm for xenon is required. Pending its determination, rough values of ρ_h were obtained by employing the reduced form of van der Waals equation and taking $\rho_c = 1.105$ gm. / cc., obtained in the present work, and $P_c = 58.89$ atm., determined by Beattie *et al.* (3). Instead of using the analytical method of Ruedy (15) a graphical method, which will also be applicable when the critical isotherm of xenon is experimentally determined, was employed in the calculations.

Starting with the critical point on the isotherm, the pressure increment $\rho_c g \delta h$ for a small height increment δh was added (or subtracted) from P_c. The density corresponding to this pressure was read off the isotherm and this new density used to calculate the pressure increment for the next height interval. The process was repeated till all the various chosen bomb lengths were included. Owing to the large density gradient at the height corresponding to ρ_c, it was necessary to take very small increments near this region; increments of 0.005 cm. were used. As the density changes became less sensitive larger intervals up to 1.0 cm. were used.

The curve showing the range of filling density, $\bar{\rho}_1 - \bar{\rho}_2$, over which the flat portion of the coexistence curve extends as a function of bomb length is given in Fig. 5. The shape of the curve indicating the rapid increase of flat-top

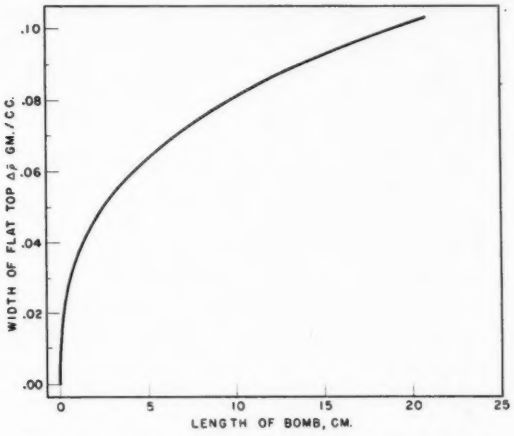

FIG. 5. Width of flat top as function of bomb length.

density range at small bomb lengths is a reflection of the fact that at small lengths most of the bomb contents are in the high density gradient region. The relevant values for the two bombs used in the present work as obtained from the curve and experimentally are as follows:

Bomb length, cm.	Density range of flat top, gm./cc.	
	van der Waals	Observed
1.2	0.039	0.025−0.07
19	0.10	0.20 −0.23

The observed values are rather uncertain for the horizontal bomb.

Thus when hydrostatic effects are taken into account, the classical van der Waals isotherm can account for a large portion of the flat-top coexistence curves observed with vertical bombs. It is highly probable that the actual critical isotherm of xenon will be considerably flatter in the critical density region and the width of the flat top of the coexistence curves calculated from it will more closely approximate to the observed widths. It would appear therefore that in a bomb of vanishing vertical length the coexistence curve will be rounded and have a definite maximum corresponding to a unique set of critical conditions. These conclusions are contrary to the theory of Mayer (10) and of Rice (14) which predict a flat-top coexistence curve in the absence of gravitational effects.

Application of the above argument to the case of sulphur hexafluoride leads

to a flat-top width well in excess of that actually observed by Atack (2). For ethylene and ethane the gravitational effect is much smaller; the experimental coexistence curve for ethylene (Naldrett and Maass (11)) has a flat top of width approximately 0.01 gm. per cc. while the width estimated as above is very roughly 0.003 gm. per cc.

Finally it should be emphasized that although gravitational effects are capable of accounting for a large part of the flat-top width of the observed coexistence curves, it is likely that other effects due to molecular clustering play a part. Such effects might be expected to vary from substance to substance. On this subject little more can be said at present until gravitational effects have been properly sorted out from the observational data.

Taking the coexistence curve determined with the horizontal bomb as an approximation to the ideal curve we may apply the Corresponding State relations of Guggenheim (5). One of these is

$$\frac{\rho_L - \rho_G}{\rho_c} = \frac{7}{2}\left(1 - \frac{T}{T_c}\right)^{\frac{1}{3}}$$

where ρ_L and ρ_G are the densities of the coexistent liquid and vapor at the absolute temperature T. Plotting $\rho_L - \rho_G$ vs. $(1 - T/T_c)^{\frac{1}{3}}$ the graph shown in Fig. 6 is obtained. The plot yields a good straight line of slope 3.65 compared to the predicted value of 3.86. The equation hence gives a fairly satisfactory representation of the present data.

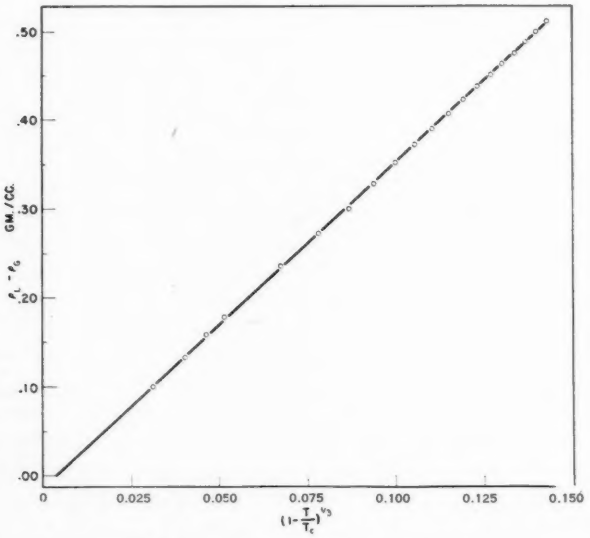

FIG. 6. Plot of $\rho_L - \rho_G$ vs. $(1 - T/T_c)^{\frac{1}{3}}$.

ACKNOWLEDGMENTS

The authors would like to express their gratitude to Mr. W. A. Stevenson for help in construction of the apparatus and Mr. G. Ensell for construction of the glass bombs. Thanks are also due to Dr. F. P. Lossing for the mass spectrometer analyses of the xenon.

REFERENCES

1. ATACK, D. and SCHNEIDER, W. G. J. Phys. & Colloid Chem. 54: 1323. 1950.
2. ATACK, D. and SCHNEIDER, W. G. J. Phys. & Colloid Chem. 55: 532. 1951.
3. BEATTIE, J. A., BARRIAULT, R. J., and BRIERLEY, J S. J. Chem. Phys. 19: 1219. 1951.
4. GOUY, G. Compt. rend. 115: 720. 1892.
5. GUGGENHEIM, E. A. J. Chem. Phys. 13: 253. 1945.
6. KAMINSKY, J. and BLAISDELL, B. E. Rev. Sci. Instruments, 10: 57. 1939.
7. MAASS, O. Chem. Revs. 23: 17. 1938.
8. MACCORMACK, K. E. and SCHNEIDER, W. G. Can. J. Chem. 29: 699. 1951.
9. MASON, S. G., NALDRETT, S. N., and MAASS, O. Can. J. Research, B, 18: 103. 1940.
10. MAYER, J. E. and HARRISON, S. F. J. Chem. Phys. 6: 87, 101. 1938.
11. NALDRETT, S. N. and MAASS, O. Can. J. Research, B, 18: 118. 1940.
12. PATTERSON, H. S., CRIPPS, R. S., and WHYTLAW-GRAY, R. Proc. Roy. Soc. (London), A, 86: 579. 1912.
13. PETERS, K. and WEIL, K. Z. physik. Chem., A, 148: 27. 1930.
14. RICE, O. K. J. Phys. & Colloid Chem. 54: 1293. 1950.
15. RUEDY, R. Can. J. Research, B, 9: 637. 1933.
16. SCHRÖER, E. Z. physik. Chem. 129: 79. 1927.

ISOTOPE EFFECTS: REACTION AT THE CARBONYL GROUP[1]

By F. Brown and D. Alma Holland

ABSTRACT

It is shown that benzophenone containing the $C^{14}O$ group reacts with 2,4-dinitrophenylhydrazine more slowly than does ordinary benzophenone. The ratio of the rate constants is 1.099± .011 at 27.8°C.

It is now well established that isotopically-distinguished molecules do not always react chemically at the same rates, differences of the order of a few per cent having been measured for carbon compounds. These effects, commonly called "isotope effects" have been observed for a number of light elements.

With carbon, isotope effects have been measured for reactions involving the breaking of both $C^{14}-C^{12}$ and $C^{14}-O$ bonds. For example Yankwich and Calvin (12) decarboxylated C^{14} malonic acid and found that the $C^{12}-C^{12}$ bond broke 12% more frequently than the $C^{14}-C^{12}$ bond. Stevens (10, 11) and co-workers have found that in the hydrolysis of esters of C^{14} benzoic acid the normal esters react about 10% faster than the C^{14} esters. He has found (9) that such isotope effects were observable only when the rate determining stage of the reaction involved a bond containing the isotopically-distinguished atom. If the isotope was in a part of the molecule other than the reacting bond, no effect was seen. Bigeleisen (1, 3, 4, 6) and Thode (7) have observed isotope effects in C^{13} compounds. Bigeleisen (2, 5) and Pitzer (8) have treated the subject from a theoretical standpoint in order to calculate isotope effects from fundamental data.

So far no work appears to have been done upon possible isotope effects in reactions involving addition to a $C^{14}-C^{12}$ or $C^{14}-O$ bond. Such an effect has now been investigated and for the purpose the reaction between benzophenone and 2,4-dinitrophenylhydrazine to give the hydrazone was chosen:

$$\mathrm{Ph-\overset{*}{C}(=O)-Ph + NH_2.NHX \rightarrow Ph-\overset{*}{C}(=N.NHX)-Ph + H_2O}$$

where X = 2,4-dinitrophenyl and the C^{14} is situated in the C = O group. Although the over-all reaction is an elimination, the rate determining stage in a reaction of this type is believed to be addition to an intermediate I.

$$\mathrm{XNH.NH_2 + \underset{\underset{\mathrm{Ph}}{|}}{\overset{\overset{\mathrm{Ph}}{|}}{C^{+}}}-OH \rightarrow XNH.N^{+}H_2-\underset{\underset{\mathrm{Ph}}{|}}{\overset{\overset{\mathrm{Ph}}{|}}{C}}-OH}$$

(I) (II)

Thus in studying this reaction we might expect to observe the isotope effect in a bond formation. It must be remembered however that very few reactions

[1] *Manuscript received December 7, 1951.*
Contribution from the Chemistry Branch, Atomic Energy Project, National Research Council of Canada, Chalk River, Ont. Issued as N.R.C. No. 2720.

consist of bond formation only, because in most cases when a bond is formed other bonds are broken or altered in some way. Thus in the above reaction the C − O bond distance will presumably alter when the C − N bond is formed; stereochemical changes will also accompany such bond formation. Furthermore if the rate controlling step of the reaction were elimination of water from (II) or the formation of (I) then we would not be observing the isotope effect in C − N bond formation.

The method by which the isotope effect may be determined for this reaction is as follows. If a mixture of C^{12} benzophenone and C^{14} benzophenone is completely converted to hydrazone then the C^{14} content per mole of the product will necessarily be the same as that of the starting material. On the other hand, when only a fraction of the benzophenone has been so converted, this initial product will have a lower C^{14} content than the parent material because the C^{14} ketone will react more slowly than the C^{12}. Conversely, the last portion of ketone to react will contain a greater proportion of C^{14} than the average.

One may consider the C^{12} ketone and the C^{14} ketone as two separate substances reacting simultaneously at slightly different rates with a third common substance, the hydrazine.

Let b = initial concentration of hydrazine.

Let a = initial concentration of C^{12} ketone and x the amount reacted in time t with velocity constant k.

Let a^1, x^1, and k^1 be the corresponding values for the C^{14} ketone at the same time.

Then the amounts of the species remaining at time t are:

$$(a - x),\ (a^1 - x^1),\ \text{and}\ (b - x - x^1).$$

Then
$$\frac{dx}{dt} = k(a - x)(b - x - x^1)$$

and
$$\frac{dx^1}{dt} = k^1(a^1 - x^1)(b - x - x^1),$$

whence
$$\frac{dx/dt}{dx^1/dt} = \frac{k(a - x)(b - x - x^1)}{k^1(a^1 - x^1)(b - x - x^1)} = \frac{k(a - x)}{k^1(a^1 - x^1)}.$$

(1)
$$\frac{k}{k^1} = \ln\frac{a}{a - x} \Big/ \ln\frac{a^1}{a^1 - x^1}$$

It will be seen that this same expression (1) will result whatever the over-all kinetic order of the reaction, provided that it is first order with respect to the ketone since in general

$$\frac{dx/dt}{dx^1/dt} = \frac{k(a - x)(b - x - x^1)(c - x - x^1)\ \text{etc.}}{k^1(a^1 - x^1)(b - x - x^1)(c - x - x^1)\ \text{etc.}} = \frac{k(a - x)}{k^1(a^1 - x^1)}.$$

The initial concentration of C^{12} ketone (a) may be obtained from the weight used, remembering that the weight of C^{14} ketone is negligible in this case. The initial concentration of C^{14} ketone (a^1) may be obtained by measuring the

C^{14} specific radioactivity of the hydrazone formed when the ketone is *completely* converted to hydrazone.

If the reaction is carried out to an extent of only 10% (for example), then the weight of hydrazone formed measures the extent of the C^{12} reaction (x) whilst the C^{14} specific radioactivity of the product enables the extent of the C^{14} reaction (x^1) to be calculated.

EXPERIMENTAL

The benzophenone containing the C^{14} = O group was synthesized by the following method:

$$Na_2C^{14}O_3 \xrightarrow[PbCl_2]{\text{heat with}} C^{14}O_2 \xrightarrow[PhMgBr]{\text{Grignard with}} PhC^{14}OOH \xrightarrow{SOCl_2} PhC^{14}OCl$$

$$\xrightarrow{AlCl_3 + C_6H_6} PhC^{14}OPh.$$

A solution of bromobenzene (1.5 ml., 2.0 gm.) in dry ether (15 ml.) was added slowly to magnesium turnings (0.35 gm.) and the mixture finally warmed in a hot water bath to complete the formation of the Grignard reagent. Meanwhile a mixture of sodium carbonate (1.0 gm.) containing C^{14} (1.0 millicurie) and lead chloride (10 gm.) was heated gently under high vacuum in order to dry it. The heat was then increased until the mixture melted and the carbon dioxide thus evolved was collected in a trap cooled by liquid nitrogen. The carbon dioxide was allowed to evaporate and then frozen into the Grignard mixture which was then warmed to room temperature and stirred with a magnetic stirrer. After one hour the whole mixture was poured onto ice and water (12 gm.) containing hydrochloric acid (1.5 ml., concentrated). The organic material was extracted twice with ether and the benzoic acid extracted from the ethereal solution with two portions of sodium bicarbonate solution. When this bicarbonate solution was acidified the benzoic acid was precipitated and was filtered off and dried. Ordinary inactive benzoic acid (1.0 gm.) was added to this precipitate which was then refluxed gently with thionyl chloride (3.5 ml.) for one hour. Three portions (15 ml.) of benzene were added successively, distilling off 10 ml. after each addition (this removes excess thionyl chloride). Inactive benzoyl chloride (1.0 gm.) and dry powdered aluminum chloride (3.5 gm.) were added and the mixture refluxed for two hours. The remaining benzene was now distilled off, ice (30 gm.) and hydrochloric acid (2 ml. concentrated) were added, and the benzophenone steam-distilled out of the mixture. The distillate was extracted three times with ether, the ether removed by evaporation, and the residual ketone distilled *in vacuo*. Inactive benzophenone (1.5 gm.) was added to the residue in the distilling flask and then distilled off in order to carry over any active benzophenone which had been left in the residue. The product was finally recrystallized from petroleum ether.

In order to determine the purity and C^{14} content of the specimen a sample was completely converted to its 2,4-dinitrophenylhydrazone by reaction with an excess of the hydrazine in alcohol. Thus in a typical experiment 2,4-dinitrophenylhydrazone (0.5 gm.) with concentrated sulphuric acid (2.0 ml.)

dissolved in water (3.0 ml.) and ethyl alcohol (15 ml.) was added to a solution of benzophenone (0.210 gm.) in alcohol (15 ml.) and the mixture left at 27.8°C. for 24 hr. All the reactions between benzophenone and the hydrazine were carried out in a thermostat at 27.8°C.

The hydrazone is practically insoluble in alcohol so that precipitation is quantitative and the precipitate may be well washed with alcohol and dried. The weight of precipitate gives a check on the purity of the material. The radioactivity was measured by recrystallizing, making a standard solution in dioxane, and pipetting 50 μl. samples onto steel disks for counting. The samples spread evenly and were so thin that self-absorption was negligible. After being dried thoroughly *in vacuo* they were counted in a Simpson type methane-filled proportional counter with an accurately reproducible geometrical efficiency of about 50%.

To determine the isotope effect the same reaction was carried out using only 10% of the hydrazine required for complete reaction. The actual extent of the reaction was obtained from the weight of precipitate formed. The activity of the product was determined, after recrystallization, in the same way as described previously.

The following precautions were taken to ensure accuracy:

(1) The determination of the complete reaction was carried out in duplicate and that of the 10% reaction in triplicate.

(2) The hydrazone samples were, as mentioned, recrystallized before counting. They were then recrystallized again and recounted. No significant change in specific activity took place.

(3) Each hydrazone sample was measured by two different observers each making at least six separate counting disks and counting each one several times.

(4) Counting rates were about 1000 counts per min. compared to a background of 70 counts per min. A C^{14} benzoic acid standard source was used frequently to check the consistency of the counting assembly. A total of more than 10,000 counts was recorded for each sample to keep the deviation due to statistical fluctuations below 1%. The contribution due to background was measured frequently (10 min.) and the counting rates of the sample corrected by an appropriate amount.

RESULTS

Reaction of C^{14} *Benzophenone with Excess 2,4-Dinitrophenylhydrazine*

Yield of hydrazone (percentage, based on weight of material used):

1st determination	84.72
2nd determination	85.78
Average (2)	85.25

Specific activity of hydrazone (counts per minute per milligram):

1st determination, 1st observer	5498	(recrystallized, 5522)
2nd observer	5491	(recrystallized, 5511)
2nd determination, 1st observer	5534	(recrystallized, 5482)
2nd observer	5545	(recrystallized, 5541)
Average (8)	5516	

NOTE: Reaction of pure (inactive) benzophenone with excess of the hydrazine gives practically 100% yield of hydrazone. It is therefore evident that the C^{14} benzophenone used in this work was not chemically pure. This does not effect the determination of the isotope effect provided that the appropriate values are used for benzophenone concentration.

Partial Reaction of C^{14} *Benzophenone with 2,4-Dinitrophenylhydrazine*

Yield of hydrazone (percentage, based on weight of material used):

1st determination	11.35
2nd determination	10.98
3rd determination	12.22
Average (3)	11.52

Specific activity of hydrazone (counts per minute per milligram):

1st determination,	1st observer	5104	
	2nd observer	4956	
2nd determination,	1st observer	5253	
	2nd observer	5111	
3rd determination,	1st observer	4998	(recrystallized, 5170)
	2nd observer	4909	(recrystallized, 4883)
Average (8)		5048	

Using the expression (1) these results give the ratio of the rate constants for ordinary C^{14} benzophenone reacting with 2,4-dinitrophenylhydrazine as:

$$\frac{k \text{ for } C^{12} \text{ benzophenone}}{k \text{ for } C^{14} \text{ benzophenone}} = 1.099 \pm .011 \text{ at } 27.8°C.$$

The error is based upon the standard deviation of the counting data. The error due to inaccuracies in estimating the extent of reaction is very small owing to the nature of the expression (1).

The isotope effect for bond formation at the carbon atom of the C = O group appears in this case to be very similar in magnitude to that observed for C − C and C − O bond ruptures.

ACKNOWLEDGMENTS

The authors wish to thank Mr. W. H. Stevens for the help of all kinds which he has given and especially for the many valuable discussions to which he has contributed. Thanks are also due to Dr. L. Yaffe who has given advice on counting techniques and has shown great interest in the work, and to Dr. A. N. Bourns of McMaster University for a valuable discussion.

REFERENCES

1. BIGELEISEN, J. J. Chem. Phys. 17: 344. 1949.
2. BIGELEISEN, J. J. Chem. Phys. 17: 425. 1949.
3. BIGELEISEN, J. and ALLEN, T. L. J. Chem. Phys. 19: 760. 1951.
4. BIGELEISEN, J. and FRIEDMAN, L. J. Chem. Phys. 17:998. 1949.
5. BIGELEISEN, J. and MAYER, M. G. J. Chem. Phys. 15: 261. 1947.
6. BOTHNER-BY, A. A. and BIGELEISEN, J. J. Chem. Phys. 19: 755. 1951.
7. LINDSAY, J. G., MCELCHERAN, D. E., and THODE, H. G. J. Chem. Phys. 17: 589. 1949.
8. PITZER, K. N. J. Chem. Phys. 17: 1341. 1949.
9. STEVENS, W. H. Private communication.
10. STEVENS, W. H. and ATTREE, R. W. Can. J. Research, B,27: 807. 1949.
11. STEVENS, W. H. and ATTREE, R. W. J. Chem. Phys. 18: 574. 1950.
12. YANKWICH, P. E. and CALVIN, M. J. Chem. Phys. 17:109. 1949.

A THEORETICAL EVALUATION OF THE NITROGEN ISOTOPE EFFECT IN THE THERMAL DEAMMONATION OF PHTHALAMIDE[1]

By Jacob Bigeleisen

ABSTRACT

A theoretical analysis is made of the effect of nitrogen isotopic substitution on the rate of deammonation of phthalamide. Good agreement is found between theory and experiment.

INTRODUCTION

In a recent study Stacey, Lindsay, and Bourns (9) have measured the fractionation of the isotopes of nitrogen in the thermal deammonation of phthalamide. The fractionation of the nitrogen isotopes in this case results from the different rates of decomposition of the isotopic phthalamide molecules. Three reactions suffice to describe the system when the isotopic composition of the nitrogen is close to natural abundance.

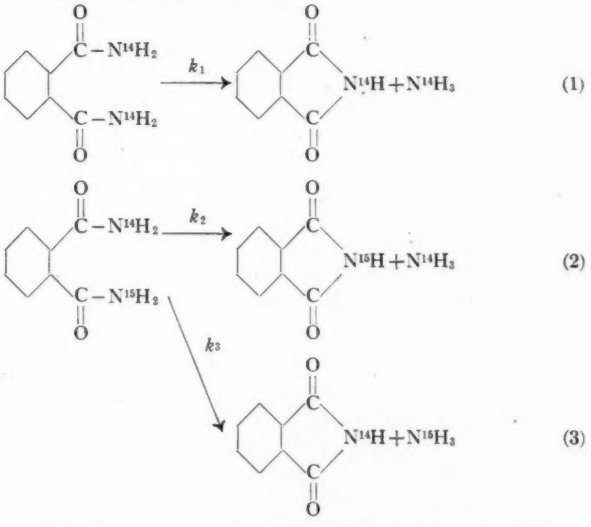

Stacey, Lindsay, and Bourns find for the ratios k_2/k_3 and $k_1/2k_2$ 1.014 ± 0.001 and 0.994 ± 0.001 respectively. They have also given a qualitative interpretation of their experimental results in terms of some cogent arguments concerning the mechanisms of the reaction and the zero point energies of the various isotopic molecules in their normal and transition states.

This paper reports the results of a somewhat more extensive theoretical analysis which does not restrict itself to the zero point energy effect alone.

[1] *Manuscript received February 7, 1952.*
Contribution from Department of Chemistry, Brookhaven National Laboratory, Upton, Long Island, New York. Research carried out under the auspices of the U. S. Atomic Energy Commission.

CALCULATIONS

The ratio of the rate constants for competitive reactions of molecules containing N^{14} and N^{15} is given by the equation (2)

$$\frac{k_{14}}{k_{15}} = \frac{S_{14}S^{\ddagger}_{15}}{S_{15}S^{\ddagger}_{14}}\frac{K_{14}}{K_{15}}\left(\frac{m^*_{15}}{m^*_{14}}\right)^{\frac{1}{2}}\left[1 + \sum_i^{3n-6} G(u_i)\Delta u_i - \sum_i^{3n'-6} G(u^{\ddagger}_i)\Delta u^{\ddagger}_i\right] \qquad (4)$$

where the subscript 14 refers to the molecule containing N^{14} and the subscript 15 refers to the molecule containing N^{15}. The other symbols have been defined previously (2). The factor involving the S's is a statistical one resulting from symmetry properties of the isotopic molecules in the normal and transition states; the factor involving the m^*'s gives the ratio of the number of molecules in the transition state decomposing per unit time; and the quantity in the square bracket on the right-hand side of Equation (4) gives a quantitative description of the zero point energy effects. The deviation of the ratio of K_{14}/K_{15} from unity can be neglected (2).

We shall first consider the ratio k_2/k_3. The factor involving the S's is unity. Since the ratio k_2/k_3 measures the relative probabilities of decomposition of one single molecular species by two paths, the term

$$\sum_i^{3n-6} G(u_i)\Delta u_i$$

is identically zero (1, 7, 8). There are strong theoretical arguments to show that

$$\sum_i^{3n'-6} G(u^{\ddagger}_i)\Delta u^{\ddagger}_i,$$

the zero point energy term in the transition state, is sufficiently close to zero that it may be safely neglected in the case where the two species being compared in the transition state are isotopic isomers (1, 5, 7, 8). The calculation of the ratio k_2/k_3 reduces, therefore, to that of the ratio $(m^*_{15}/m^*_{14})^{\frac{1}{2}}$.

For the calculation of the ratio k_2/k_3 we must consider only that phase of the reaction where the geometry of the molecule is changed so that the two amide nitrogen atoms are no longer equivalent. If we suppose, for instance, that they become distinguished by the attachment of an electron to one of the carbonyl groups, then the isotopic composition of the ammonia and phthalimide resulting from complete reaction will be identical. This results from the fact that we have distinguished the two nitrogen atoms by a process which is independent of the mass of the nitrogen atom and a subsequent reaction carried to completion will give a product of the same isotopic composition as the substrate (3, 4).

For a bond involving a given pair of atoms the value of m^* is independent of whether or not the bond is being formed or broken. This statement can be easily understood if we consider the exchange reaction of isotopes of an element B

$$A - B' + B = AB + B' \qquad (5)$$

which we shall assume proceeds through the mechanism

$$A - B' \underset{k_{6r}}{\overset{k_{6f}}{\rightleftharpoons}} A + B' \tag{6}$$

$$A - B \underset{k_{7r}}{\overset{k_{7f}}{\rightleftharpoons}} A + B \tag{7}$$

$$K_5 = K_6/K_7 = \frac{k_{6f}}{k_{7f}} \Big/ \frac{k_{6r}}{k_{7r}} \tag{8}$$

If we designate the primed atom as the light atom, then

$$K_5 = f_{AB} = \frac{Q_{AB}}{Q_{AB'}} \left(\frac{m_{B'}}{m_B}\right)^{3/2} \tag{9}$$

where f is the reduced partition function ratio defined by Bigeleisen and Mayer (6), Q is the total partition function of the molecule, and $m_{B'}$ and m_B are the masses of B' and B respectively.

Since
$$\frac{k_{6f}}{k_{7f}} = \left(\frac{m^*_{7f}}{m^*_{6f}}\right)^{1/2} \frac{K_{6f}}{K_{7f}} \, f_{AB}/f^{\ddagger}_{AB} \tag{10}$$[2]

and
$$\frac{k_{6r}}{k_{7r}} = \frac{K_{6r}}{K_{7r}} \left(\frac{m^*_{7r}}{m^*_{6r}}\right)^{1/2} \frac{1}{f^{\ddagger}_{AB}} \tag{11}$$

then
$$K_5 = f_{AB} = f_{AB} \left(\frac{m^*_{7f}}{m^*_{6f}}\right)^{1/2} \frac{K_{6f}}{K_{7f}} \Big/ \left(\frac{m^*_{7r}}{m^*_{6r}}\right)^{1/2} \frac{K_{6r}}{K_{7f}} \tag{12}$$

or
$$\left(\frac{m^*_{7f}}{m^*_{6f}}\right)^{1/2} \frac{K_{6f}}{K_{7f}} = \left(\frac{m^*_{7r}}{m^*_{6r}}\right)^{1/2} \frac{K_{6r}}{K_{7r}} . \tag{13}$$

The derivation of Equation (13) can be generalized to include any number of atoms in the molecule without any loss in rigor. In the present case the ratios of the transmission coefficients are unity and

$$\frac{m^*_{7f}}{m^*_{6f}} = \frac{m^*_{7r}}{m^*_{6r}} .$$

From the fact that k_2/k_3 is different from unity we must conclude that the destruction of the symmetry in the phthalamide molecule on deammonation does not involve the simultaneous formation and rupture of C–N bonds. We shall assume, as seems reasonable, that the destruction of symmetry involves the rupture of one C–N bond and an increase in the bond strength of the other C–N bond. Additional evidence for this model will be presented in our discussion of the ratio $k_1/2k_2$. This model leads to the value of 1.016 for $(m^*_{15}/m^*_{14})^{\frac{1}{2}}$ and for k_2/k_3.[3] Stacey, Lindsay, and Bourns give the following values for k_2/k_3 from their nitrogen analyses of the ammonia.

[2] *See Equation (5) Ref. (2).*
[3] *The method of calculation is discussed in Reference (8).*

TABLE I

INTRAMOLECULAR ISOTOPE EFFECT IN THE DEAMMONATION OF PHTHALAMIDE[4]

Exp't.	k_2/k_3
D–H–1	1.009
D–H–3	1.015
D–H–7	1.014
D–H–10	1.016
D–H–11	1.014
D–H–12	1.015

They consider these values more reliable than those obtained from the isotopic analyses of the nitrogen in the phthalimide. The agreement between theory and experiment is very satisfactory.

We shall now consider the ratio $k_1/2k_2$ with the above-mentioned model. In this case Equation (4) reduces to

$$\frac{k_1}{2k_2} = 1 + \sum_i^{3n-6} G(u_i)\Delta u_i \; - \sum_i^{3n'-6} G(u_i^\ddagger)\Delta u_i^\ddagger . \qquad (14)$$

According to the convention adopted in the definition of $G(u)$ both

$$\sum_i^{3n-6} G(u_i)\Delta u_i \text{ and } \sum_i^{3n'-6} G(u_i^\ddagger)\,\Delta u_i^\ddagger$$

are positive numbers. Their magnitude for compounds containing the isotopes of nitrogen at 450°K. is of the order 0.00-0.06. We have previously postulated for our model of the transition state a situation where one C–N bond is lengthened (this nitrogen forms NH_3) and one C–N bond is shortened. In comparing Equations (1) and (2) we see that in both cases a C^{12}–N^{14} bond is lengthened. Therefore

$$\sum_i^{3n'-6} G(u_i^\ddagger)\Delta u_i^\ddagger > \sum_i^{3n-6} G(u_i)\Delta u_i$$

and we predict that phthalamide containing one N^{15} will liberate $N^{14}H_3$ somewhat faster than does phthalamide containing N^{14} alone. This is in agreement with experiment. Furthermore we can estimate that this difference should be less than 3%, which is also in agreement with experiment. More detailed calculations would hardly be justified for a molecule of this complexity and with our present paucity of information about the nature of the potential in the region of the transition state.

ACKNOWLEDGMENT

I wish to thank Messrs. Stacey, Lindsay, and Bourns for giving me a copy of their manuscript in advance of publication.

[4] *Data of Stacey, Lindsay, and Bourns (9).*

REFERENCES

1. BIGELEISEN, J. J. Chem. Phys. 17: 425. 1949.
2. BIGELEISEN, J. J. Chem. Phys. 17: 675. 1949.
3. BIGELEISEN, J. Science, 110: 14. 1949.
4. BIGELEISEN, J., BOTHNER-BY, A. A., and FRIEDMAN, L. Brookhaven National Laboratory Report BNL 44, p. 39 (To be published shortly).
5. BIGELEISEN, J. and FRIEDMAN, L. J. Chem. Phys. 17: 998. 1949.
6. BIGELEISEN, J. and MAYER, M. G. J. Chem. Phys. 15: 261. 1947.
7. BOTHNER-BY, A. A. and BIGELEISEN, J. J. Chem. Phys. 19: 755. 1951.
8. FRIEDMAN, L. and BIGELEISEN, J. J. Chem. Phys. 18: 1325. 1950.
9. STACEY, F. W., LINDSAY, J. G., and BOURNS, A. N. Can. J. Chem. 30: 135. 1952.

THE PREPARATION OF SODIUM CHLORIDE OF LARGE SPECIFIC SURFACE[1]

By A. Craig[2] and R. McIntosh

ABSTRACT

A procedure is outlined by which sodium chloride particles of specific surface up to 50 m.^{2} per gm. may be prepared. The particles form in chains and are found to lose area rapidly in moist air. The fundamental units of the chain do not appear cubic. Single cubic particles or chains of cubic particles also have been prepared. The one sample identified as this type had a specific surface of 18 m.^{2} per gm. The sintering in moist air appears to occur by a process of solution and recrystallization. A value of the interfacial free energy solid–liquid is calculated from the data.

INTRODUCTION

The preparation of nonporous solids of simple crystalline form and of large specific surface is of importance in carrying out studies of physically adsorbed gases. For example, the determination of the specific heat (10) or the dielectric constant (8) of the adsorbate requires the use of adsorbents of large area per gram. The extension of measurements such as those made by Lipsett, Johnson, and Maass (7), by which the total surface energy of the solid is determined, necessitates the use of readily soluble crystals of large and known specific surface. The area of any preparations of sodium chloride used in these studies or for gas adsorption was about 3 m.^{2} per gm. or less. It has been found possible to prepare sodium chloride having a specific surface as high as 50 m.^{2} per gm. with simple apparatus. Such material is formed in chains, and the ultimate particles may well be amorphous rather than crystalline (see Fig. 1). However, cubic material of 18 m.^{2} per gm. has also been prepared (see Fig. 3) and it may well be possible to prepare such particles of appreciably higher specific surface. The mass concentration of sodium chloride vapor in the carrier gas stream and careful maintenance of anhydrous conditions throughout the preparation are important factors in obtaining the high surface areas. Thus material of large specific surface may have been formed in the experiments of earlier workers (6,7), but rapid sintering due to the presence of water vapor would have reduced the area of the final product to the comparatively low values reported. Data are presented below which suggest that sintering occurs by dissolution and recrystallization. The effect of water vapor on small particles of sodium chloride had already been discerned by McLauchlan, Sennett, and Scott (9) through examination of particles which had been prepared in small quantity by evaporation *in vacuo*. The electron microscope was employed, and readily observable changes in the size of the particles were noted after exposure to the air in the room.

[1] *Manuscript received January 14, 1952.*
Contribution from the Department of Chemistry, University of Toronto, Toronto, Ont. Based on a thesis submitted as partial fulfillment of the requirements for the degree of Master of Arts in the Graduate School of the University of Toronto.
[2] *Present address: Polymer Corporation, Sarnia, Ontario.*

No attempt is made here to establish the mechanism of formation of the particles, for two reasons. First, the material obtained in the precipitator, the surface area of which was determined, amounted to 50% by weight of the sodium chloride evaporated. Second, the lack of reproducibility of specific surface for a given set of conditions suggests that some sintering by water vapor occurred and was still a factor of some importance in the procedure described below.

EXPERIMENTAL

The powders were prepared by evaporating sodium chloride contained in a porcelain boat in a tube furnace. The carrier gas was dried air passed at a rate of 4.2 liters per min. at room temperature through a silica tube of 2.6 cm. internal diameter. Temperatures were varied between 750°C. and 850°C. An arrangement was provided for removing the plug of coarse salt which accumulated at the exit end of the tube and which accounted for 20% of the sodium chloride which was evaporated. The smoke particles were collected in an alternating current electrostatic precipitator. This was made from 25 mm. outside diameter Pyrex tubing. The precipitating chamber was 31 cm. in length. A tungsten wire along the axis of the tube served as one electrode, and a sheet of aluminum foil, wound around the outside of the tube and earthed, formed the other electrode (3,6). A potential difference of 20,000 volts from a 64 kv. transformer controlled by a Variac precipitated all the powder. At the completion of an experiment the particles which had been collected in the precipitator were scraped carefully into a small container of about 20 cc. capacity designed to form the sample holder of a standard type of adsorption apparatus (4). In the early experiments no care was taken to maintain anhydrous conditions during the transfer of the powder. This omission resulted in widely varying specific surfaces of the products and no area greater than 15 $m.^2$ per gm. was found. In later experiments the removal of the powder from the precipitator was carried out under a stream of dried air and was performed as rapidly as possible. The samples were transferred and most of the air had been pumped from the dead space of the adsorption apparatus within about 10 min. after production had been stopped. Unless this evacuation is performed immediately, the powder cannot be stored in a desiccator without loss of area.

After evacuation at room temperature for 24 hr. to a pressure of 10^{-6} mm. of Hg, the total surface area was measured by adsorption of carbon dioxide at -78.5°C. The adsorption data were plotted according to the Hüttig adsorption equation (5) as the results gave better linear plots than when the BET multilayer formula (2) was employed. Adsorption of carbon dioxide was reversible, and repetition of an adsorption isotherm after evacuation at room temperature was closely reproducible. The main source of uncertainty in assigning relative values of the area was the selection of the linear section of the plot, which resulted in 3.5% uncertainty between duplicate tests. For areas of about 3 $m.^2$ the reproducibility was 10%, while for areas of 30 $m.^2$ the reproducibility was 4%. The area found using carbon dioxide was checked with one sample by the use of nitrogen at the normal boiling point of nitrogen.

The area found in two tests was appreciably larger than that obtained by the use of carbon dioxide, namely 60 m.^{2} per gm. as compared with 40 m.^{2} per gm. Thus the values of area reported are lower than would be assigned if nitrogen had been used in the determinations. Rough estimates of specific surface from the electron microscope photographs of the cubic type particles (see Fig. 3) and of a sample which had sintered in the presence of water vapor (see Fig. 2) are not inconsistent with the magnitudes of the specific surface values given.

In the case of the cubic particles shown in Fig. 3, if the two single particles are taken to have the average dimensions of all the ultimate particles, the calculated specific surface from the dimensions of the particles is 20 m.^{2} per gm. The value obtained by the gas adsorption method is 17.8 m.^{2} per gm. In the case of the sintered particles of Fig. 2, if the particle of intermediate size in the center of the figure is treated as a sphere and assumed to be the "average" particle, a specific surface of 6.3 m.^{2} per gm. is obtained taking a mean radius of 0.22 microns. If it is treated as an oblate ellipsoid and assumed to be the "average" particle, a specific surface of 6.2 m.^{2} per gm. results. The value from the gas adsorption measurement is 9.0 m.^{2} per gm. Clearly these comparisons are approximate as no attempt was made to examine a large number of particles and to average the total area obtained. In addition no account is taken of any surface which would arise from indentations or porosity.

Only sodium chloride was revealed by spectrographic tests of the products. Chemical tests revealed the presence of a small amount of sulphuric acid, about sufficient to cover 0.3 m.^{2} per gm. with a single molecular layer. This impurity apparently was carried from the drying towers as dispersed material in the carrier gas. Because of the small quantities involved and because the sintering phenomena discussed below are known to occur when no hygroscopic contaminant such as sulphuric acid could be present (9), it is not believed that the presence of the sulphuric acid is the cause of the behavior on exposure to water vapor.

RESULTS

The results of some of the experiments are summarized in Table I.

The yield in all experiments was 50% in the electrostatic precipitator and independent of mass concentration. The uncertainty in the mass balance was 5%.

In view of the irregularity of the specific surface found for a given mass concentration, it does not appear reasonable to assign a value of concentration for maximum specific surface. Although an interdependence is revealed between mass concentration and specific surface of product whereas none was discernible before exposure to water vapor was at least partially controlled, there remains sufficient lack of reproducibility to suggest that the effect of moisture has not been completely eliminated.

A series of experiments designed to confirm the effect of exposure to moist air was carried out. After the initial determination of specific surface, the powder sample was transferred to a desiccator in which a known relative

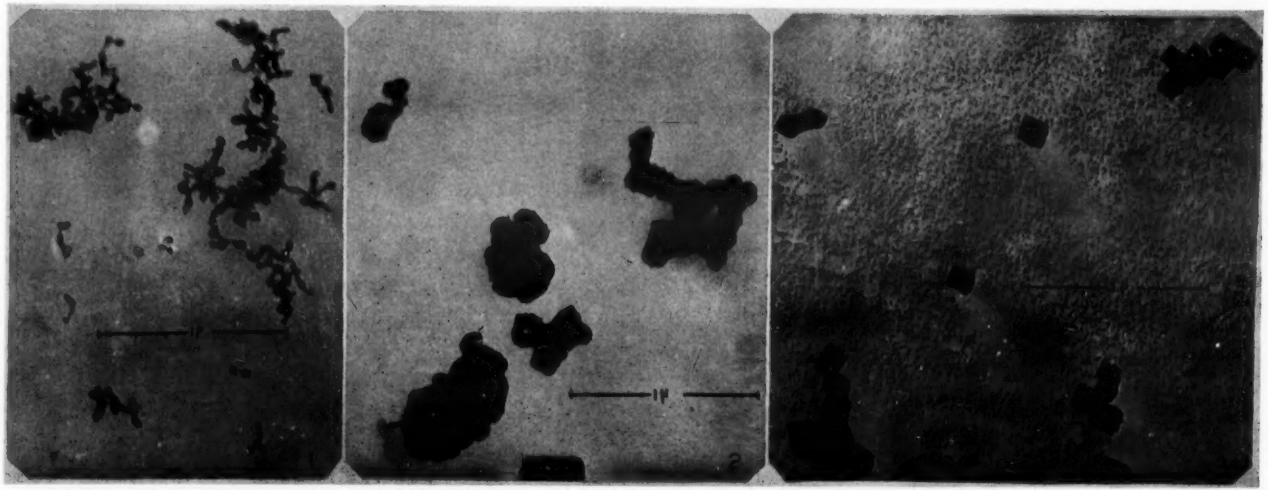

FIG. 1. Sodium chloride particles of specific surface 51.8 m.² per gm.
FIG. 2. Sodium chloride particles after exposure to water vapor. Area 9.0 m.² per gm.
FIG. 3. Cubic type sodium chloride particles of specific surface 17.8 m.² per gm.

TABLE I

THE EFFECT OF CONCENTRATION OF NaCl VAPOR ON THE SPECIFIC SURFACE

Sample No.	Mass concentration in mgm. NaCl per liter of air at 23°C. × 10^2	Area, $m.^2/gm.$
31	1.95	33.7
32	14.4	7.1
35	4.54	24.5
36	1.69	54.4
37	2.22	32.7
38	1.11	47.3
39	2.48	43.4
40	6.84	23.5
41	6.00	44.4
42	7.50	20.4
43	1.13	51.8
44	8.78	17.8*

* *Cubic particles or chains of cubic particles (See Fig. 3).*

TABLE II

THE EFFECT OF MOIST AIR ON THE SPECIFIC SURFACE

Initial area, $m.^2/gm.$	Relative pressure of water vapor	Duration of exposure, hr.	Final area, $m.^2/gm.$
24.5	.05	24	21.7
44.4	.05	240	14.4
23.5	.05	240	18.2
21.7	.15	273	8.4
47.3	.15	203	9.0
43.4	.25	95	3.2

pressure of water vapor was maintained by means of a solution of sulphuric acid and water (12). After known periods the sample was again pumped free of gases and the area redetermined.

Although the number of observations is small, to a first approximation two results seem evident. First, the final value of specific surface is lower the higher the relative pressure to which the powder is exposed. Second, the final value of specific surface is independent of the initial value of the surface area. Both of these observations are consistent with the postulate that sintering occurs by a process of dissolution at certain parts of the surface, and recrystallization to form a surface from which no further dissolution occurs. When no further diminution of surface is observed at a given relative pressure, apparently all parts of the surface have a surface free energy and curvature such that no further changes take place. The particles might then be considered as particles which could remain in contact with a water solution of the salt the vapor pressure of which is that partial pressure of water vapor to which the particles were exposed. From such data and the assumption of spherical particles, the interfacial free energy of the solid–liquid interface can be computed from the well-known relation

$$\ln \frac{a_{\text{part}}}{a_{\text{bulk}}} = \frac{2\bar{V}\sigma_{sl}}{r'RT}.$$

where a_{part} is the activity of the salt in the solution saturated with respect to the finely divided material and a_{bulk} is the activity of the salt in a solution saturated with respect to large crystals. Unfortunately, values of the activities of sodium chloride in highly supersaturated solutions are not available. Estimates of these values have been made by the use of Equation 11*a* of Stokes and Robinson (11), using the constants given for lithium chloride and sodium hydroxide. Neither set of constants gives the correct value of the molality of the saturated sodium chloride solution if the known activity of water in the saturated solution is used in Equation 11*a*. The error is in the direction to give large values of σ_{sl}. From the known molality of a saturated sodium chloride solution one may also obtain the activity of the water from Equation 11*a*. These values will give somewhat lower figures for σ_{sl}, but not appreciably lower. The results tabulated in Table III were all obtained using the experimental value for the activity of water in the saturated solution and the molality obtained with Equation 11*a*.

TABLE III

VALUES OF THE INTERFACIAL FREE ENERGY OF THE SOLID–LIQUID INTERFACE

Salt	Constants of Equation 11*a*		Interfacial free energy in ergs/cm.^{2} from data at various relative pressures		
	c	*r*	.05	.15	.25
LiCl	17.2	3.64	4.8×10^4	6.9×10^4	1.3×10^5
NaOH	19.3	3.20	4.2×10^4	6.0×10^4	1.5×10^5

The values are higher by a factor of 10 than those usually quoted (1). Part of the discrepancy is undoubtedly due to the oversimplification of the spherical model of the particles. Part may be due to high values of the activity of the salt in supersaturated solutions given by the equation 11*a*. In addition to these causes there is perhaps the amorphous character which may obtain for the surface, and an effect, here neglected, due to the presence of the minute quantity of sulphuric acid.

It is interesting to note that on the basis of the theory loss of area occurs by a solution process, it must be supposed that multilayers of water, capable of dissolving salt, are established on those areas attacked. Presumably one acceptable hypothesis is the formation of liquid water by capillary condensation in narrow channels, but these would be extremely narrow for even the highest relative pressure of 0.25 (less than 10 Å). Further investigation is required to clarify such points of interest.

ACKNOWLEDGMENT

It is a pleasure to acknowledge our indebtedness to Mr. Woodward and Professor Scott of the Physics Department for the electron microscope photographs and to the Advisory Committee on Research of the University of Toronto for financial aid.

REFERENCES

1. ADAM, N. K. The physics and chemistry of surfaces. Oxford University Press. 1941. p. 199.
2. BRUNAUER, S., EMMETT, P. H., and TELLER, E. J. Am. Chem. Soc. 60: 309. 1938.
3. DRINKER, P. J. Ind. Hyg. 14: 364. 1932.
4. EMMETT, P. H. Advances in colloid science, Vol. 1. Interscience Publishers, Inc., New York. 1942.
5. HÜTTIG, G. F. Monatsh. 78: 177. 1948.
6. KEENAN, A. G. and HOLMES, J. M. J. Phys. & Colloid Chem. 53: 1309. 1949.
7. LIPSETT, S. G., JOHNSON, F. M. G., and MAASS, O. J. Am. Chem. Soc. 49: 925. 1927.
8. MCINTOSH, R. L., RIDEAL, E. K., and SNELGROVE, J. A. Proc. Roy. Soc. (London), A, 208: 292. 1951.
9. MCLAUCHLAN, T. A., SENNETT, R. S., and SCOTT, G. D. Can. J. Research, A, 28: 530. 1950.
10. MORRISON, J. A., LOS, J. M., and DRAIN, L. E. Trans. Faraday Soc. 47: 1023. 1951.
11. STOKES, R. H. and ROBINSON, R. A. J. Am. Chem. Soc. 70: 1870. 1948.
12. WILSON, R. E. Ind. Eng. Chem. 13: 326. 1921.

THE PREPARATION OF *p*-BROMOPHENACYL ESTERS AND THE CHARACTERIZATION OF *p*-BROMOPHENACYL FORMATE[1]

By A. C. Neish and R. U. Lemieux

ABSTRACT

The compound, m.p. 140°C., widely used as a derivative for the identification of formic acid was found to be *p*-bromophenacyl alcohol and not *p*-bromophenacyl formate. *p*-Bromophenacyl alcohol was also the product from an attempt to prepare *p*-bromophenacyl pyruvate. *p*-Bromophenacyl formate, m.p. 92°C., was prepared in 80% yield by refluxing equivalent amounts of the reactants in 66% alcohol for 30 min. This ester is readily hydrolyzed under the conditions used for its preparation and the hydrolysis appears to be catalyzed by salts of carboxylic acids. The melting point of *p*-bromophenacyl alcohol depended on the rate of heating, varying from 137°C. with slow heating to 142°C. with the rapid heating obtained on a melting point bar.

Judefind and Reid (6) first used the reaction between *p*-bromophenacyl bromide and the sodium salts of carboxylic acids for preparing crystalline derivatives suitable for identification of the acids. This is an excellent method particularly for identifying small amounts of volatile acids since the aqueous solution of the salts can be evaporated and then taken up in dilute alcohol for the reaction. The yields are good and the derivatives show a marked increase in weight over the original acid. A method of obtaining formic acid as a crystalline compound suitable for its identification and for measurements of carbon-14 activity was needed in this laboratory. The *p*-bromophenacyl ester was judged to be the most suitable after examining the literature, because of its relatively high melting point and apparent ease of preparation.

Judefind and Reid (6) were unable to obtain a crystalline derivative of formic acid. However, Hurd and Christ (5) had no difficulty in obtaining a crystalline compound, m.p. 140°C., which they reported to be *p*-bromophenacyl formate. This compound is listed as such in tables of derivatives (10, p. 222) and has been widely used to identify formic acid.

The most frequently described conditions for the preparation of *p*-bromophenacyl esters prescribe the use of about four equivalent weights of sodium salt for each mole of *p*-bromophenacyl bromide and a reflux period of one to two hours. When this procedure was used to prepare the formic ester from sodium formate labeled with carbon-14, the compound melting at 140°C. was readily obtained; actually it melted at 142°C. with rapid heating on the Dennis melting point bar (2). However, the substance was *nonradioactive*. Analysis for the elements indicated that the compound was probably *p*-bromophenacyl alcohol. A sample of authentic *p*-bromophenacyl alcohol was prepared by hydrolysis of *p*-bromophenacyl acetate using the procedure of Judefind and Reid (6). The authentic alcohol melted at 142°C. and this melting point was unchanged on admixture with the reaction product of *p*-bromophena-

[1] *Manuscript received January 21, 1952.*
Contribution from the Prairie Regional Laboratory, National Research Council, Saskatoon, Sask. Issued as N.R.C. No. 2719.

cyl bromide and excess sodium formate. The two compounds possessed identical infrared absorption spectra (see Fig. 1).

On attempting to prepare *p*-bromophenacyl formate using equivalent amounts of reactants, we obtained a new compound, m.p. 92°C. The yield was 86% after a reflux period of 30 min. and 45% after heating for one hour. The substance possessed the elementary composition expected for *p*-bromophenacyl formate and, when prepared from carbon-14 labeled sodium formate, the product had the intensity of radioactivity expected from the activity of the sodium formate used.

It is thus established that the compound previously reported (6) as *p*-bromophenacyl formate is in fact *p*-bromophenacyl alcohol. *p*-Bromophenacyl

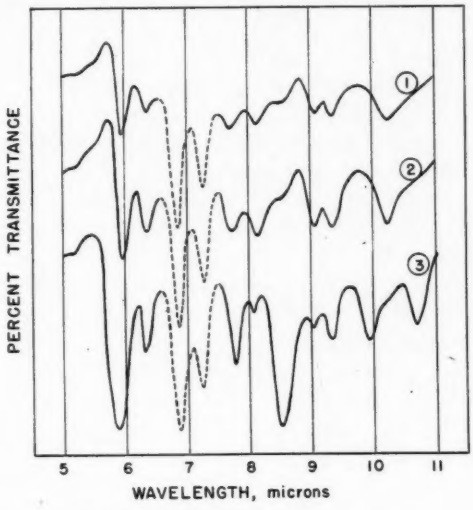

FIG. 1. Infrared absorption spectra.
Curve 1. Authentic *p*-bromophenacyl alcohol, m.p. 142°C.
Curve 2. Compound, m.p. 142°C., from reaction of *p*-bromophenacyl bromide with excess sodium formate.
Curve 3. *p*-Bromophenacyl formate, m.p. 92°C.

formate melts at 92°C. and is further characterized by its infrared spectrum shown in Fig. 1.

Langenbeck and Baehren (7) have shown that phenacyl esters undergo hydrolysis with exceptional ease. The esters of formic acid and α-ketoacids are well known (10, p. 65) to be highly sensitive to hydrolytic conditions. It therefore would be expected that phenacyl esters for formic acid and α-keto-acids, such as pyruvic acid, would be exceptionally prone to hydrolysis. When *p*-bromophenacyl formate was treated for 80 min. with an equivalent amount of either sodium formate or sodium acetate under the temperature and pH conditions used for the preparation of the ester, the substance was hydrolyzed in high yield (80-90%) to *p*-bromophenacyl alcohol, but it was recovered

unchanged (78% yield) under the same conditions if the carboxylic salts were omitted. Thus, the hydrolysis of the ester appears to be catalyzed by salts of carboxylic acids. On treating *p*-bromophenacyl acetate with sodium formate in aqueous alcohol, the acetate was recovered unchanged, m.p. 85°C., yield 74%. *p*-Bromophenacyl pyruvate like the formate is readily hydrolyzed by the conditions used for its preparation. When *p*-bromophenacyl bromide was treated with four equivalents of sodium pyruvate under the usual conditions for the preparation of *p*-bromophenacyl esters, *p*-bromophenacyl alcohol was isolated as a reaction product in 81% yield. The pyruvic ester appears to be formed less quickly and to be more sensitive to hydrolysis than the formic ester since, under the conditions which gave high yields of the formate, only unreacted *p*-bromophenacyl bromide and *p*-bromophenacyl alcohol could be readily isolated from the reaction product. It is possible that in the past certain acids such as pyruvic acid may have been mistaken for formic acid because of the characterization of the latter acid using *p*-bromophenacyl alcohol as a derivative.

Drake and Bronitsky (3) found that *p*-phenylphenacyl esters are suitable derivatives for acids such as formic acid. However, they used conditions similar to those which we have found suitable for the preparation of *p*-bromophenacyl formate and it seems probable that their superior results are due more to the procedure used rather than the reagent. In general it is to be recommended for the preparations of *p*-substituted phenacyl esters that equivalent amounts of reactants be used and that the reaction time be kept to a minimum.

It is of interest to note that the procedure recently introduced by Erickson *et al.* (4) for the preparation of *p*-bromophenacyl esters by reaction of *p*-bromo-α-diazoacetophenone with the acid in dioxane apparently gives crude *p*-bromophenacyl alcohol when formic acid is used.

EXPERIMENTAL

Chemicals

Radioactive sodium formate was prepared by hydrogenation of sodium bicarbonate using palladium black as the catalyst (11). *p*-Bromophenacyl bromide was made following the directions of Langley (8) and recrystallized to a constant melting point of 109°C. *p*-Bromophenacyl acetate was prepared in the usual way (6).

Methods

Melting points were determined using the Dennis melting point apparatus (2) as manufactured by the Parr Instrument Co. This apparatus was calibrated against several pure compounds with known melting points each time it was used. The results are corrected melting points accurate to about 0.5°C.

The activity of barium carbonate and *p*-bromophenacyl formate labeled with carbon-14 was determined using a windowless counter operating with helium–isobutane in the Geiger region. Appropriate resolving-time corrections were made and all results referred to a cellulose acetate standard, of the same area, which was made from carbon-14 labeled cellulose. The samples were

mounted by filtration on disks of Whatman No. 3 paper using a special funnel which ensured uniform distribution and constant surface area (9). Successive mounts made from the same material did not usually differ by more than 2-4% (9). Activity determinations were made using "infinitely thick" samples.

p-Bromophenacyl Formate

Ten milliliters of molar sodium formate was made acid to phenol red by dropwise addition of 0.10 *N* hydrochloric acid. Ethanol (20 ml.) and *p*-bromophenacyl bromide (2.8 gm.) were added and the mixture refluxed gently for 30 min. It was then evaporated to about 15 ml. on a steam bath and cooled in refrigerator. The crystals were filtered off, washed with a little aqueous ethanol (20%), then with water, and dried at room temperature. The yield was 2.1 gm. (86%) of colorless leaflets melting at 91.5°C. Recrystallization from ethanol–petroleum raised the melting point to 92°C. A similar experiment using a reflux time of one hour gave a yield of 1.1 gm. (45%).

Calculated for $C_9H_7O_3Br$:	C = 44.47%	H = 2.90%	Br = 32.87%
Found:	C = 44.34%	H = 3.01%	Br = 33.65%

p-Bromophenacyl Formate from C^{14} Labeled Sodium Formate

A molar sodium formate solution was prepared from formate labeled with carbon-14. One aliquot (0.5 ml.) was oxidized to carbon dioxide by refluxing with mercuric oxide (3 gm.), water (25 ml.), and syrupy phosphoric acid (5 ml.). The carbon dioxide was trapped in *N* sodium hydroxide, precipitated as barium carbonate (1), and its activity measured. Another aliquot (3 ml.) was converted to the *p*-bromophenacyl ester using the same proportions as above. The activity of the ester was measured after recrystallizing to constant melting point and activity. A portion of this pure ester was then converted to barium carbonate using the Van Slyke combustion fluid (12) and its activity again measured. The activities found were as follows (counts per minute at infinite thickness):

$BaCO_3$ from oxidation of sodium formate	11,840
p-Bromophenacyl formate	9560
$BaCO_3$ from oxidation of *p*-bromophenacyl formate	1345

These values are in excellent agreement with those expected for a compound with the formula $C_9H_7O_3Br$ containing one carbon derived from the formate. Thus the equivalent weight with respect to formate carbon is $197 \times 11{,}840/9560 = 243$, which coincides with the theoretical value. The activity of the barium carbonate obtained on oxidation of this ester should be $11{,}840/9 = 1315$. The value found above agrees within the experimental error (2-4%) for mounting active barium carbonate samples (9).

Preparations of p-Bromophenacyl Alcohol

Ten milliliters of 5*N* sodium formate was made acid to phenol red by dropwise addition of 0.01 *N* hydrochloric acid. Ethanol (20 ml.) and *p*-bromophenacyl bromide (2.8 gm.) were added and the mixture refluxed gently for one hour. After concentrating to half volume and cooling in refrigerator 1.5 gm. (70%) of crystals melting at 140°C. was obtained. Recrystallization from alcohol and toluene–petrol ether gave 1.1 gm. of needles melting at 142°C.

Calculated for $C_8H_7O_2Br$: C = 44.67% H = 3.28% Br = 37.16%
Found: C = 44.76% H = 3.31% Br = 36.35%

When prepared as above using carbon-14 labeled sodium formate this compound was obtained free of radioactivity, indicating absence of formate carbon in the molecule.

Determination of the molecular weight by the Rast method (using camphor) gave successive readings, on heating and cooling the same sample, corresponding to molecular weights of 412, 320, 283, 243, 224, and 220. The calculated value ($C_8H_7O_2Br$) is 214.9. Another experiment gave an initial weight of 545 decreasing gradually to 189 over a period of two and one-half hours' heating.

A sample of *p*-bromophenacyl alcohol was prepared by the method of Judefind and Reid (6). After recrystallizing from water and then from toluene it was obtained with the same melting point (142°C.) as the product of the reaction between *p*-bromophenacyl bromide and excess sodium formate. A mixture of the two melted at 142°C. The melting point seems to depend on the rate of heating. A sample heated slowly (15 min. for the last 10°) in a capillary tube melted at 137-136.5°C., in close agreement with the value of 136.6°C. reported by Judefind and Reid (6). However, the determination of the melting point with a heating time of about one second using the Dennis melting point apparatus (2) gave the above indicated melting point of 142°C. Comparison of the infrared spectra shown in Fig. 1 also shows these two samples of *p*-bromophenacyl alcohol to be identical.

The molecular weight determinations recorded above show a gradual decrease from an initial high value close to that expected for a monomer. This suggests that *p*-bromophenacyl alcohol, like acetoin, is associated in the crystalline state by a linkage which slowly dissociates on heating. The dependence of the melting point on the rate of heating also supports this view.

Relative Stability of the Formyl and Acetyl Esters of p-Bromophenacyl Alcohol

Two millimoles of *p*-bromophenacyl formate and *p*-bromophenacyl acetate in 4 ml. of ethanol were treated separately with 2 ml. of a molar solution of sodium formate made acid to phenol red. After refluxing for 80 min., the resulting acidic solution was concentrated to half volume and cooled. The *p*-bromophenacyl acetate was recovered unchanged, m.p. 85°C., yield 74%. The *p*-bromophenacyl formate was converted to *p*-bromophenacyl alcohol, m.p. 142°C. in 86% yield. When the sodium formate solution was replaced by water *p*-bromophenacyl formate was recovered in 78% yield from the resulting acidic reaction mixture. One millimole of sodium acetate, 82 mgm., was dissolved in 1 ml. of water and the solution was made acid to phenol red by dropwise addition of 0.01 *N* hydrochloric acid. To the resulting solution 243 mgm. of *p*-bromophenacyl formate, 1 mM., and 2 ml. of ethanol were added and the mixture was refluxed for 80 min. The reaction mixture was diluted with 1 ml. of water and cooled. The crystalline product, 192 mgm., washed with water and air dried, melted at 138.5-140.5°C. and this melting point was not depressed by admixture of *p*-bromophenacyl alcohol.

Attempted Preparations of p-Bromophenacyl Pyruvate

A molar solution of sodium pyruvate was made acid to phenol red by the dropwise addition of 0.1 *N* hydrochloric acid. Ten milliliters of the solution was added to 2.8 gm., 10 mM., of *p*-bromophenacyl bromide in 20 ml. of ethanol and the mixture was refluxed for a half hour. On cooling at about 4°C. for two hours, the solution deposited crystals which after recrystallization from ethanol melted at 108-109°C. and this melting point was not depressed by admixture of *p*-bromophenacyl bromide. The yield was 0.50 gm. The combined filtrates were evaporated *in vacuo* to about 15 ml. The air-dried precipitate which formed weighed 1.98 gm. This material was dissolved in 6 ml. of boiling ethanol and, on cooling to room temperature, 0.27 gm. of a crystalline material, m.p. 125-136°C., was deposited. Recrystallization of this substance from toluene and then from ethanol gave a product, m.p. 140-141.5°C. The melting point was not depressed by mixing with *p*-bromophenacyl alcohol. Ten milliliters of the acidic sodium pyruvate solution was added to 0.70 gm., 2.5 mM., of *p*-bromophenacyl bromide in 20 ml. of ethanol and the solution was refluxed for two hours. The resulting solution was evaporated *in vacuo* to about 15 ml. and cooled. The crystals which formed were washed with 20% ethanol and air dried. Recrystallization from 4 ml. of ethanol gave 0.39 gm., 72% yield, of material, m.p. 140.5-141.5°C. The melting point was not depressed by admixture of *p*-bromophenacyl alcohol.

ACKNOWLEDGMENTS

The valuable technical assistance provided by Miss Carol Brice and J. A. Baignee is gratefully acknowledged.

REFERENCES

1. CALVIN, M., HEIDELBERGER, C., REID, J. C., TOLBERT, B. M., and YANKWICH, P. F. Isotopic carbon. John Wiley & Sons, Inc., New York. 1949. Chap. 6.
2. DENNIS, L. M. and SHELTON, R. S. J. Am. Chem. Soc. 52: 3128. 1930.
3. DRAKE, N. L. and BRONITSKY, J. J. Am. Chem. Soc. 52: 3715. 1930.
4. ERICKSON, J. L. E., DECHARY, J. M., and KESLING, M. R. J. Am. Chem. Soc. 73: 5301. 1951.
5. HURD, C. H. and CHRIST, R. E. J. Am. Chem. Soc. 57: 2007. 1935.
6. JUDEFIND, W. L. and REID, E. E. J. Am. Chem. Soc. 42: 1043. 1920.
7. LANGENBECK, W. and BAEHREN, F. Ber. 69: 514. 1936.
8. LANGLEY, W. D. *In* Organic syntheses. Collective Vol. 1. John Wiley & Sons, Inc., New York. 1932. p.127.
9. NEISH, A. C. and SPYKER, J. W. Unpublished work. Details will be sent on request.
10. SHRINER, R. L. and FUSON, R. C. Identification of organic compounds. 3rd ed. John Wiley & Sons, Inc., New York. 1948.
11. SPYKER, J. W. and NEISH, A. C. Can. J. Chem. In Press.
12. VAN SLYKE, D. D. and FOLCH, J. J. Biol. Chem. 136: 509. 1940.

CANADIAN JOURNAL OF CHEMISTRY

Notice to Contributors

GENERAL: Manuscripts should be typewritten, double spaced, and the **original and one extra copy** submitted. Style, arrangement, spelling, and abbreviations should conform to the usage of this Journal. Names of all simple compounds, rather than their formulas, should be used in the text. Greek letters or unusual signs should be written plainly or explained by marginal notes. Superscripts and subscripts must be legible and carefully placed. Manuscripts should be carefully checked before being submitted, to reduce the need for changes after the type has been set. If authors require changes to be made after the type is set, they will be charged for changes that are considered to be excessive. **All pages, whether text, figures, or tables, should be numbered.**

ABSTRACT: **An abstract of not more than about 200 words, indicating the scope of the work and the principal findings, is required.**

ILLUSTRATIONS:

(i) *Line Drawings:* All lines should be of sufficient thickness to reproduce well. Drawings should be carefully made with India ink on white drawing paper, blue tracing linen, or co-ordinate paper **ruled in blue only;** any co-ordinate lines that are to appear in the reproduction should be ruled in black ink. Paper ruled in **green, yellow, or red should not be used** unless it is desired to have all the co-ordinate lines show. Lettering and numerals should be neatly done in India ink preferably with a stencil (**do not use typewriting**) and be of such size that they will be legible and not less than one millimeter in height when reproduced in a cut three inches wide. All experimental points should be carefully drawn with instruments. Illustrations need not be more than two or three times the size of the desired reproduction, but the ratio of height to width should conform with that of the type page. **The original drawings and one set of small but clear photographic copies are to be submitted.**

(ii) *Photographs:* Prints should be made on glossy paper, with strong contrasts; they should be trimmed to remove all extraneous material so that essential features only are shown. Photographs should be submitted **in duplicate;** if they are to be reproduced in groups, one set should be so arranged and mounted on cardboard with rubber cement; the duplicate set should be unmounted.

(iii) *General:* **The author's name, title of paper, and figure number should be written in the lower left hand corner (outside the illustration proper) of the sheets on which the illustrations appear.** Captions should not be written on the illustrations, but typed together at the end of the manuscript. All figures (including each figure of the plates) should be numbered consecutively from 1 up (arabic numerals). **Each figure should be referred to in the text.** If authors desire to alter a cut, they will be charged for the new cut.

TABLES: Each table should be typed on a separate sheet. Titles should be given for all tables, which should be numbered in Roman numerals. Column heads should be brief and textual matter in tables confined to a minimum. **Each table should be referred to in the text.**

REFERENCES: **These should be listed alphabetically by authors' names, numbered in that order, and placed at the end of the paper.** The form of literature citation should be that used in this Journal. **Titles of papers should not be given.** The first page only of the references cited should be given. **All citations should be checked with the original articles.** Each citation should be referred to in the text by means of the key number.

REPRINTS: A total of 50 reprints of each paper without covers are supplied free to the authors. Additional reprints will be supplied according to a prescribed schedule of charges. On request, covers can be supplied at cost.

Approximate charges for reprints may be calculated from the number of printed pages, obtained by multiplying by 0.6 the number of manuscript pages (double-spaced typewritten sheets, 8½ in. by 11 in.) and making allowance for space occupied by line drawings and halftones (not inserts). The cost per page is tabulated at the back of the reprint request form sent with the galley.

Contents

Page

The Flow of Fluids Through Activated Carbon Rods. III. The Flow of Adsorbed Fluids—*E. A. Flood, R. H. Tomlinson, and A. E. Leger* - 389

1-Indoleacetic Acid—*W. S. Smith and R. Y. Moir* - - - - - - - 411

On the Liquid–Vapor Coexistence Curve of Xenon in the Region of the Critical Temperature — *M. A. Weinberger and W. G. Schneider* - 422

Isotope Effects: Reaction at the Carbonyl Group—*F. Brown and D. Alma Holland* - - - - - - - - - - - - - - - - - - 438

A Theoretical Evaluation of the Nitrogen Isotope Effect in the Thermal Deammonation of Phthalamide—*Jacob Bigeleisen* - 443

The Preparation of Sodium Chloride of Large Specific Surface—*A. Craig and R. McIntosh* - - - - - - - - - - - - - - - - 448

The Preparation of *p*-Bromophenacyl Esters and the Characterization of *p*-Bromophenacyl Formate—*A. C. Neish and R. U. Lemieux* - 454

Printed in Canada *by* University of Toronto Press